2. EXPLANATORY NOTES[1]

Shipboard Scientific Party[2]

Standard procedures for drilling operations and preliminary shipboard analysis of the material recovered have been regularly amended and upgraded since 1968 during investigations conducted by the Deep Sea Drilling Project (DSDP) and the Ocean Drilling Program (ODP). This chapter presents information to help the reader understand the data-gathering methods on which our preliminary conclusions are based and to help shore-based investigators select samples for further analysis. This information concerns primarily shipboard operations and analyses described in the Leg 117 site reports (this volume). Preliminary results from shipboard analysis of each individual site are given in the site chapters.

AUTHORSHIP OF SITE REPORTS

Authorship of the site reports is shared among the entire scientific party. The scientists responsible for a particular field also contributed for their specific area of study. Because of the heavy work load of the sedimentologists and biostratigraphers, a senior sedimentologist and senior biostratigrapher were responsible for compiling and editing the "Lithostratigraphy" and "Biostratigraphy" sections for each site chapter. The site chapters are organized as follows (authorship in parentheses):

Site Summary (Prell, Niitsuma, Emeis)
Background and Objectives (Prell, Niitsuma, Emeis)
Operations (Emeis)
Lithostratigraphy (Anderson, Clemens, Debrabant, Krissek, Murray, Niitsuma, Ricken, al Sulaimani, al Tobbah, Weedon)
Biostratigraphy (Hermelin, Kroon, Nigrini, Spaulding, Takayama)
Paleomagnetism (Bloemendal, Hayashida, de Menocal, al Tobbah)
Accumulation Rates (Murray, Niitsuma)
Interhole and Intersite Correlations (de Menocal, Niitsuma)
Physical Properties (Bilak, Bush, Bray)
Seismic Stratigraphy (Jarrard, Prell, Ricken)
Inorganic Geochemistry (Pedersen, Shimmield)
Organic Geochemistry (Emeis, ten Haven)
Downhole Measurements (Barnes, Jarrard)
Summary and Conclusions (Prell, Niitsuma)

Following the text are summaries ("barrel sheets") of the lithologic core descriptions and the biostratigraphic and magnetostratigraphic results and photographs of each core.

SURVEY AND DRILLING DATA

The survey data used to locate the site are discussed in the individual site chapters. En route between sites and upon arrival in the target areas, continuous observations were made of water depth and sub-bottom structure. Site surveys using a precision depth recorder (PDR) and seismic profiler were made aboard *JOIDES Resolution* before dropping the beacon. Equipment used and single-channel seismic-reflection data collected during Leg 117 are presented in the "Underway Geophysics" chapter (this volume).

Bathymetric data were obtained with both 3.5- and 12-kHz PDR echo-sounders, using a Raytheon PTR-105B transceiver and 12 Raytheon transducers for the 3.5-kHz data. Two Raytheon LSR-1807M recorders were used for display. Depths were read on the basis of an assumed 1463 m/s sound velocity. Water depth (in meters) at each site was corrected (1) according to the tables of Matthews (1939) and (2) for the depth of the hull transducer, 6 m below sea level. In addition, depths referred to the drilling platform are assumed to be 10.5 m above the water line.

DRILLING CHARACTERISTICS

Because water circulation down the hole is open, drill cuttings are lost onto the seafloor and cannot be recovered. The only information about characteristics of strata in uncored or unrecovered intervals, other than from seismic data or wireline-logging results, is from the rate of drilling penetration. Typically, the harder the layer, the slower and more difficult it is to penetrate. However, other factors that are not directly related to the hardness of the layers also determine the rate of penetration, including the parameters of bit weight, pump pressure, and revolutions per minute, all of which are noted on the drilling recorder.

DRILLING DEFORMATION

When cores are split, some show signs of significant sediment disturbance. Examples of this disturbance include the downward-concave bending of originally horizontal layers, the haphazard mixing of lumps of different lithologies, and the near-fluid state of some sediments recovered from tens to hundreds of meters below the seafloor. Core deformation probably occurs during one of three different steps: cutting, retrieval (with accompanying changes in pressure and temperature), and core handling.

SHIPBOARD SCIENTIFIC PROCEDURES

Numbering of Sites, Holes, Cores, and Samples

ODP drill sites are numbered consecutively from the first site drilled by *Glomar Challenger* in 1968. A site number refers to one or more holes drilled while the ship is positioned over a single acoustic beacon. Several holes may be drilled at a single site by pulling the drill pipe above the seafloor (out of one hole), moving the ship some distance from the previous hole, and then drilling another hole.

For all ODP drill sites, a letter suffix distinguishes each hole drilled at the same site. For example: the first hole takes the site number with suffix A, the second hole takes the site number with suffix B, and so forth. This procedure is different from that used by DSDP (Sites 1–624) but prevents ambiguity between site and hole number designations.

[1] Prell, W. L., Niitsuma, N., et al., 1989. *Proc. ODP, Init. Repts.*, 117: College Station, TX (Ocean Drilling Program).

[2] Shipboard Scientific Party is as given in the list of Participants preceding the contents.

All ODP core and sample identifiers indicate core type. The following abbreviations are used: R = rotary core barrel (RCB), H = advanced hydraulic piston core (APC), P = pressure core barrel, X = extended core barrel (XCB), B = drill-bit recovery, C = center-bit recovery, I = *in-situ* water sample, S = sidewall sample, W = wash core recovery, N = Navidrill core (used from Leg 104 on), and M = miscellaneous material. APC, XCB, RCB, I, and W were employed on Leg 117.

The cored interval is measured in meters below seafloor. The depth interval of an individual core is the depth below seafloor that the coring operation began to the depth that the coring operation ended. Each coring interval is as much as 9.7 m long, which is the maximum length of a core barrel. The coring interval may, however, be shorter. Cored intervals are not necessarily adjacent but may be separated by drilled intervals. In soft sediment, the drill string can be "washed ahead," keeping the core barrel in place but not recovering sediment, by pumping water down the pipe at high pressure to wash the sediment out of the way of the bit and up the annulus between the drill pipe and wall of the hole. However, if thin, hard rock layers are present, it is possible to get "spotty" sampling of these resistant layers within the washed interval.

Cores taken from a hole are numbered serially from the top of the hole downward (Fig. 1). Maximum full recovery from a single core is 9.7 m of sediment or rock in a plastic liner (6.6 cm inner diameter), plus a sample about 0.2 m long (without a plastic liner) in a core catcher (CC). The core catcher, a device at the bottom of the core barrel, prevents the core from sliding out when the barrel is retrieved from the hole. The sediment core, in the plastic liner, is cut into 1.5-m-long sections, which are numbered serially from the top of the core. With full recovery, the sections are numbered from 1 through 7, the last section being shorter than 1.5 m. For sediments and sedimentary rocks, the core-catcher sample is placed below the last section and treated as a separate section. For igneous and metamorphic rocks, material recovered in the core catcher is included at the bottom of the last section.

When recovery is less than 100%, whether or not the recovered material is contiguous, the recovered sediment is placed at the top of the cored interval, and then 1.5-m-long sections are numbered serially, starting with Section 1 at the top. There are as many sections as needed to accommodate the length of the core recovered. Sections are cut starting at the top of the recovered sediment, and the last section may be shorter than the normal 1.5-m length. If, after the core has been split, fragments that are separated by a void appear to have been contiguous *in situ*, a note is made in the description of the section. All voids, whether real or artificial, are curatorially preserved. We made an effort to compute depth below seafloor in cores with gas voids by collapsing the voids. Depths thus computed are given in the "Samples" column of the barrel sheets for Sites 723 and 724.

Sample locations are designated by distances in centimeters from the top of each section to the top and bottom of the sample. A full identification number for a sample consists of the following information: (1) leg, (2) site, (3) hole, (4) core number and type, (5) section, and (6) interval in centimeters. For example, the sample identification number "117-721A-3H-2, 98–100 cm" indicates that a sample was taken between 98 and 100 cm from the top of Section 2 of APC-drilled Core 3, from the first hole (A) drilled at Site 721 during Leg 117. A sample taken from between 8 and 9 cm in the core catcher of this core would be designated "117-721A-3H, CC (8–9 cm)." In the case of recovery less than or equal to 100%, the depth below seafloor of a given sample is calculated as follows: depth below seafloor of the top of the core (tabulated in the "Operations" section for each site) plus 1.5 m for each complete section plus the distance

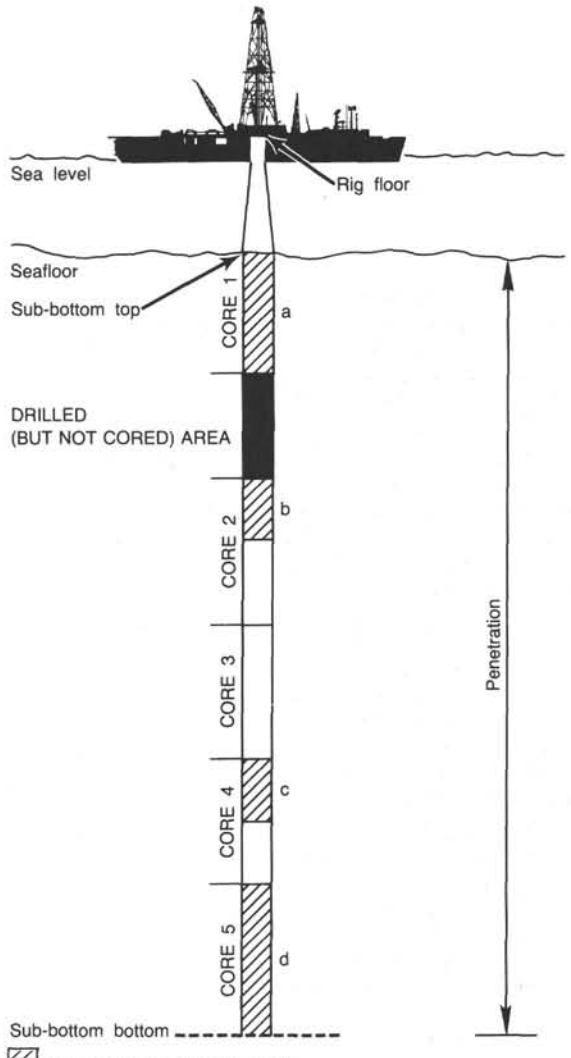

Figure 1. Numbering of core sections and terms used in coring operations and core recovery.

of the sample from the top of the sampled section. For example, the sub-bottom depth of Sample 117-721B-9H-5, 98–100 cm, is 83.38 m below seafloor (mbsf): 76.4 m (top of Core 117-721B-9H given in the Site 721 coring summary) plus 6.0 m (four complete (1.5-m) sections) plus 0.98 m (depth from top of Section 5). Sample depths given in this volume are given with two digits, even though such accuracy may be fictitious. Sample requests should refer to specific intervals, however, rather than to sub-bottom depths. Note that this assignment of subseafloor depth is an arbitrary convention; in the case of less than 100% recovery, the sample could have come from any interval within the cored interval.

Because of the gaseous nature of the organic-rich sediments of the Oman margin, core expansion resulting from decompression during core retrieval was a common phenomenon on Leg 117. Cores from Sites 723 and 724 in particular expanded significantly, giving rise to "recoveries" in excess of 110%, when voids separated sediment intervals. For example, Core 117-723A-35X drilled the interval from 321.5 to 326.3 mbsf (4.8 m), but voids developed in the core liner and pushed the sediment out of the liner. The voids were recorded in the barrel sheets so that the total length of the "recovered" section was 5.93 m, or 123% recovery. A uniform, though arbitrary, sub-bottom depth notation for samples from these expanded cores with a "recovered" section significantly longer than the cored interval (i.e., cores with greater than 105% recovery) is noted in the "Samples" column of the barrel sheets as collapsed depth in m below seafloor, following the subtraction of void space.

Core Handling

As soon as a core was retrieved on deck, a sample was taken from the core catcher and sent to the paleontological laboratory for an initial assessment of the age of the sample.

Next, the core was placed on the long horizontal rack on the catwalk, and gas samples were taken by piercing the core liner and withdrawing gas into a vacuum-tube sampler. Voids within the core were sought as sites for gas sampling. Most of the gas samples were analyzed immediately as part of the shipboard safety and pollution-prevention program. The core then was marked into section lengths; each section was labeled, and the core was cut into sections. Interstitial-water (IW) and organic geochemistry (OG) whole-round samples were taken as scheduled. Each section was sealed top and bottom with a plastic cap, blue to identify the top of a section and clear for the bottom. A yellow cap was placed on section ends from which a whole-round core sample had been removed. The caps were usually attached to the liner by coating the end of the liner and the inside rim of the end caps with acetone, though we elected to tape the end caps in place without acetone where geochemistry samples were taken on Leg 117.

The cores were then carried into the laboratory, and the complete identification was engraved on each section. The length of core in each section and the core-catcher sample was measured to the nearest centimeter; this information was logged into the shipboard core-log data base program.

Cores from some holes were allowed to warm to a stable temperature (approximately 3 hr) before splitting. During this time, the whole-round sections were run through the gamma ray attenuation porosity evaluator (GRAPE) device for estimating bulk density and porosity (see "Physical Properties" section, this chapter; Boyce, 1976), the *P*-wave logger (PWL), and the magnetic susceptibility apparatus. Owing to the large number of cores handled at some sites on Leg 117, it was not always possible to run every section through the GRAPE and PWL. After the temperature of the cores had reached equilibrium, thermal conductivity measurements were made immediately before splitting (see "Physical Properties" section, this chapter). Again, at "busy" sites, thermal conductivity could not be measured for every section. In this case, a measurement strategy was determined prior to each site.

Cores were split lengthwise into working and archive halves. The softer cores were split with a wire, and the harder ones with a band saw or diamond saw. In soft sediments, some smearing of material can occur. To minimize contamination, scientists avoided sampling the near-surface part of the split core.

The working half of the core was sampled for both shipboard and shore-based laboratory studies. Each extracted sample was logged in the sampling computer program by location and the name of the investigator receiving the sample. Records of all removed samples are kept by the ODP Curator at Texas A&M University. The extracted samples were sealed in plastic vials or bags and labeled with a computer-printed label.

The archive half was described visually. Smear slides were made from samples taken from the archive half, and thin sections were made from the working half. The archive half of each core was photographed after description with both black-and-white and color film.

Both halves were then put into labeled plastic tubes, sealed, and transferred to cold-storage space aboard the drilling vessel. Leg 117 cores were shipped from Mauritius in refrigerated containers to cold storage at the ODP Gulf Coast Repository at Texas A&M University, College Station, Texas.

At several sites on Leg 117, triple APC holes were drilled through the top 200 m of the sediment column to enable the implementation of extended whole-round sampling programs. The cores remaining after these samples were taken were not split (except where additional stratigraphic information was required) but were frozen and transported to the repository for ODP core preservation and aging studies. Unfortunately, they were accidentally thawed in port, which may limit their use as pristine samples for geochemical investigation.

SEDIMENT CORE DESCRIPTION FORMS ("BARREL SHEETS")

The core description forms (Fig. 2), or barrel sheets, summarize the data obtained during shipboard analysis of each core. The following discussion explains the ODP conventions used in compiling the data for each part of the core description form and exceptions from the standardized format necessitated by peculiarities of the sediments recovered during Leg 117.

Core Descriptions

Cores are designated using leg, site, hole, and core number and type as previously discussed (see "Numbering of Sites, Holes, Cores, and Samples," this chapter). In addition, the cored interval is specified in terms of meters below sea level (mbsl) and mbsf. Leg 117 mbsl depths are based on PDR measurements, whereas mbsf depths are drill-pipe measurements reported by the SEDCO Coring Technician and the ODP Operations Superintendent.

Age Data

Biostratigraphic zone assignments, as determined by shipboard paleontologists, appear on the core descriptions form under the heading "Biostratigraphic Zone/Fossil Character." Preservation and abundance of fossil groups are treated in the "Biostratigraphy" sections of the site chapters. An asterisk (*) denotes the location of samples taken from the core catcher or from the core. "Barren" signifies that no fossils of the particular group were recognized in the sample. Geologic age determined from the paleontological and/or paleomagnetic results noted in the "Time-Rock Unit" column. Detailed information on the zonations and terms used to report abundance and preservation appears in the "Biostratigraphy" section (this chapter).

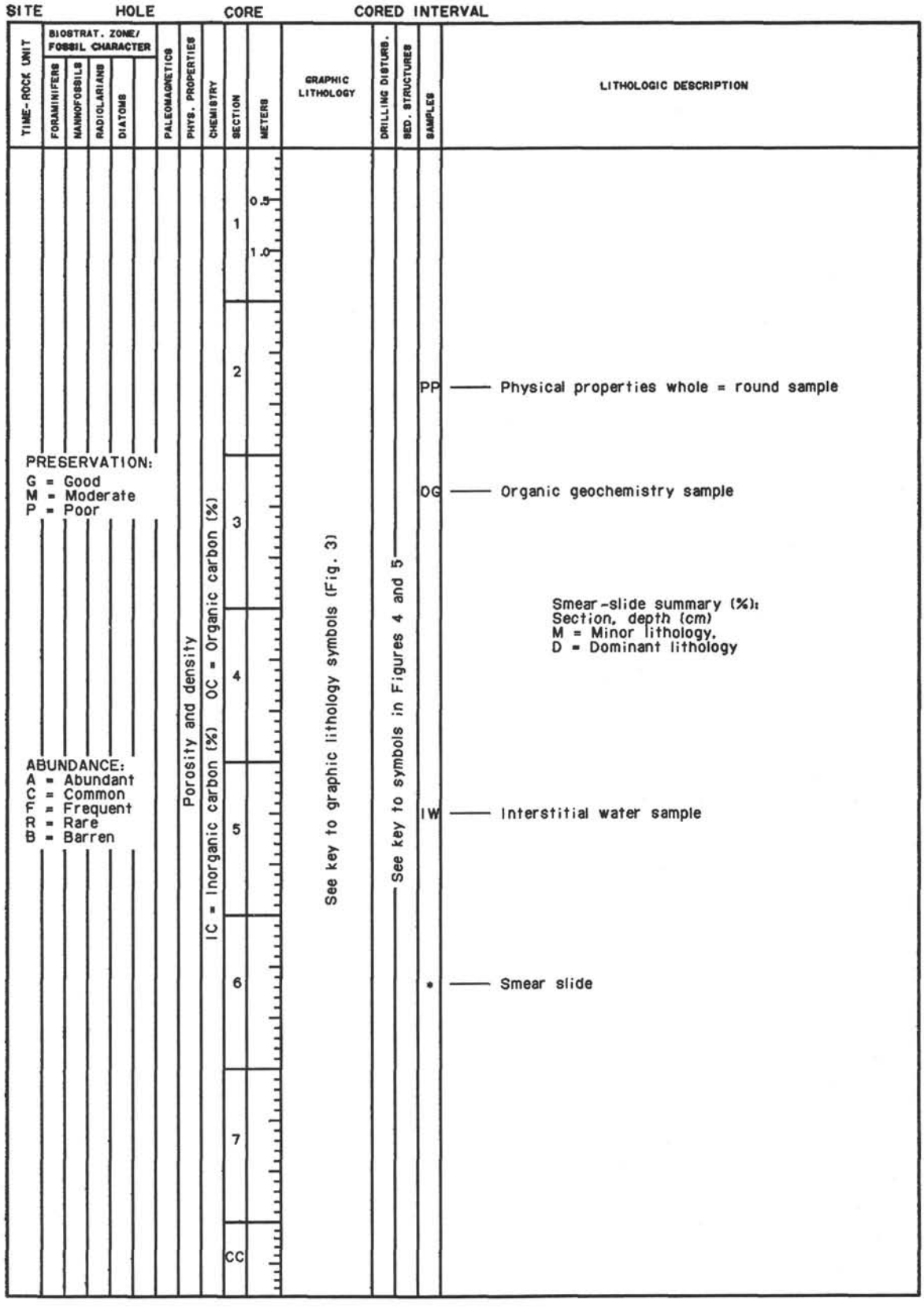

Figure 2. Core description form (barrel sheet) used for sediments and sedimentary rocks.

Paleomagnetic, Physical Properties, and Chemical Data

Columns are provided on the core description form to record paleomagnetic results, location of the physical-properties samples, and shipboard results for undrained shear strength (γ) and porosity (ϕ), as well as results of inorganic carbon (IC) and organic carbon (OC) measurements on splits of squeezed sediments from interstitial-water or carbonate bomb samples. Information on shipboard procedures for collecting these types of data is in the "Physical Properties," "Paleomagnetics," and "Organic Geochemistry" sections of this chapter. Detailed results of these and other sample analyses are given in the respective sections for each site, as well as tabulated results of calcium carbonate concentrations in the "Lithostratigraphy" sections.

Graphic Lithology

Lithologies are shown on the core description form by one or more of the symbols shown in Figure 3. The symbols correspond to end-members of the sediment compositional range, such as nannofossil ooze (CB1) or diatom ooze (SB1). For sediments that are mixtures (e.g., clastic and biogenic sediments), the symbols for both constituents are shown divided by a dashed line. For interbedded sediments, the symbols are separated by a solid line. In each case, the abundance of each constituent approximately equals the percentage of the width of the graphic column that its symbol occupies. For example, if the left 20% of the column has a nannofossil ooze symbol (CB1) and the right 80% has a clay symbol (T1) separated by a dashed line, the sediment is a mixture of 80% clay and 20% calcareous nannofossils. A solid line separating the symbols would indicate that the lithology consists of interbedded clay and diatom ooze. Minor lithologies are noted in the "Lithologic Description" space but not in the "Graphic Lithology" column where they are less than 10 cm in thickness. At some sites, core expansion was severe and resulted in voids in the core liners. For these cases, the depth labels in the voids in the "Graphic Lithology" column of the core description form correspond to the depth below seafloor of the top of the following sediment interval with the void collapsed.

Drilling Disturbance

Recovered rocks and soft sediments may be slightly to extremely disturbed. The condition of disturbance is indicated in the "Drilling Disturbance" column on the core description forms. The symbols for the six disturbance categories used for soft and firm sediments are shown in Figure 4. The disturbance categories are defined as follows:

1. Slightly disturbed or fractured: Bedding contacts are slightly bent or disturbed by fractures.
2. Moderately disturbed or fractured: Bedding contacts have undergone extreme bowing, and firm sediment has been broken into drilling biscuits 5 to 10 cm in length.
3. Very disturbed or highly fragmented: Bedding is completely disturbed or homogenized by drilling, sometimes showing symmetrical diapirlike structure in softer sediments.
4. Soupy: Water-saturated intervals have lost all aspects of original bedding.
5. Brecciated: Indurated sediment broken into angular fragments by the drilling process, perhaps along preexisting fractures.

Sedimentary Structures

The locations and types of sedimentary structures in a core are shown by graphic symbols in the "Sedimentary Structures" column in the core description form. Figure 5 gives the key for these symbols. Horizontal dashed lines denote gradational boundaries between light and dark layers or subtle compositional changes. It should be noted, however, that in some cases (mostly in deeper sections) it is difficult to distinguish between natural structures and structures created by the drilling process.

Lithologic Description of Sediments

The sediment classification scheme that is used on Leg 117 is a modified version of the sediment classification system devised by the JOIDES Sedimentary Petrology and Physical Properties Panel (SP4) and adopted for use by the JOIDES Planning Committee in March, 1974. The classification scheme used on Leg 117 incorporates many of the suggestions and terminology of Dean et al. (1985). This classification scheme is descriptive rather than generic in nature—that is, the basic sediment types are defined on the basis of their texture and composition, rather than on the basis of their inferred origin. The texture and composition of sediment samples and the areal abundances of grain components were commonly estimated by the examination of smear slides with a petrographic microscope; thus, they may differ from more accurate measurements of texture and composition, especially for coarser grained sediments. The composition of some sediment samples was determined by more accurate methods, such as coulometer or X-ray diffraction analyses, in the shipboard laboratories.

General Rules of Classification

Every sample of sediment is assigned a main name that defines its sediment type, a major modifier(s) that describes the compositions and/or textures of grains present in abundances from 10% to 100%, and possibly a minor modifier(s) that describes the compositions and/or textures of grains that are present in abundances from 5% to 10%. Grains that are present in abundances from 0% to 5% are considered insignificant and are not included in this classification.

The minor modifiers are listed first in the string of terms that describes a sample and are attached to the suffix "-bearing," which distinguishes them from major modifiers. When two or more minor modifiers are employed, they are listed in order of increasing abundance. The major modifiers are always listed second in describing a sample, and they are listed in order of increasing abundance also. Some major modifiers are attached to the suffix "-rich", whereas others are not (e.g., diatomaceous vs. nannofossil-rich). The main name is the last term in the descriptive string.

The types of main names and modifiers that are employed in this classification scheme differ between the three basic sediment types (Table 1), and are described in the succeeding sections.

Color

Sediment colors are determined by comparison with the Geological Society of America Rock-Color Chart (Munsell Soil Color Charts, 1971). Colors were determined immediately after the cores were split and while they were still wet.

Smear Slide Summary

Smear slide/thin-section compositions and the section and centimeter intervals of all samples are listed below the core description. In addition, the sample locations in the cores are indicated by an asterisk in the "Samples" column on the core description forms.

BASIC SEDIMENT TYPES: DEFINITIONS

Three basic sediment types are defined on the basis of variations in the relative proportions of clastic, siliceous biogenic, and calcareous biogenic grains: clastic sediments, siliceous bio-

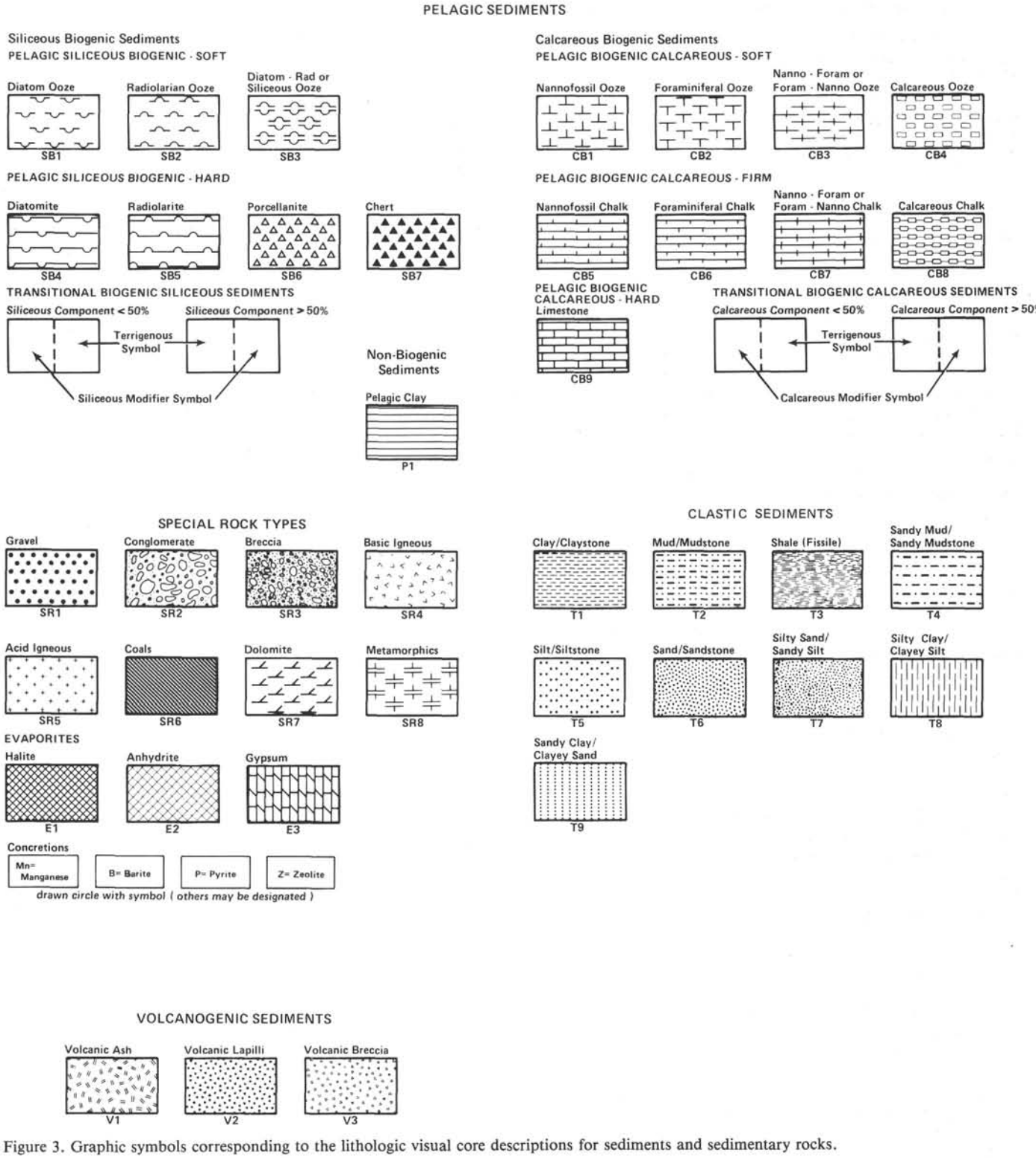

Figure 3. Graphic symbols corresponding to the lithologic visual core descriptions for sediments and sedimentary rocks.

genic sediments, and calcareous biogenic sediments (Fig. 3 and Table 1).

Clastic Sediments

Clastic (terrigenous) sediments are composed of greater than 30% terrigenous grains (i.e., rock and mineral fragments), less than 30% calcareous grains, and less than 10% siliceous biogenic and authigenic grains.

The main name for a clastic sediment describes the textures of the clastic grains and its degree of consolidation. The Wentworth (1922) grain-size scale (Table 2) is used to define the textural class names for clastic sediments. A single textural class name (e.g., "sand," "silt," or "clay") is used when one textural class is present in abundance exceeding 80%. When two or more textural classes are present in abundances greater than 20%, they are listed in order of increasing abundance (e.g., "silty

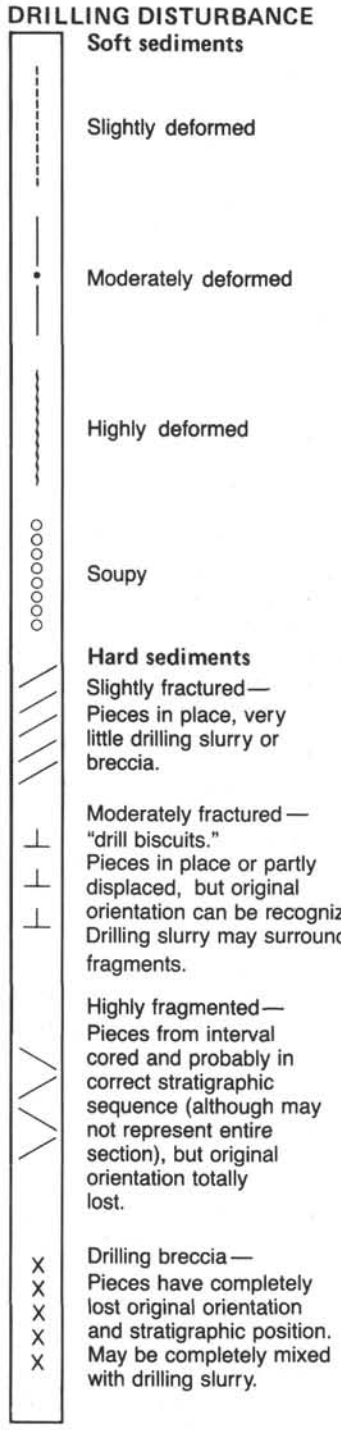

Figure 4. Drilling disturbance symbols used on Leg 117 core description forms.

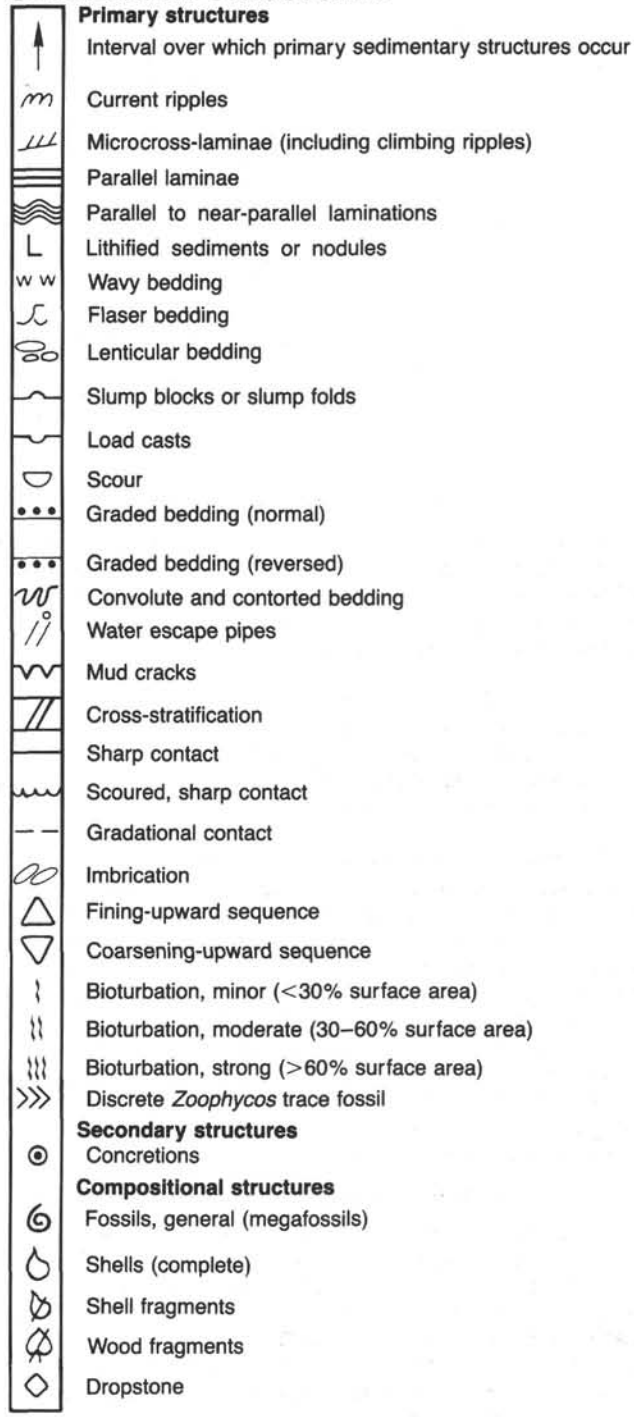

Figure 5. Sedimentary structure symbols for sediments and sedimentary rocks.

sand" or "silty clay"). The term "mud" is restricted to mixtures of sand, silt, and clay, with greater than 20% and less that 60% of each textural class (Fig. 6).

The major and minor modifiers for a clastic sediment describe the compositions of the clastic grains as well as the compositions of accessory biogenic grains. The compositions of terrigenous grains can be described by terms such as "quartz," "feldspar," "glauconite," or "lithic" (for rock fragments). The major clastic components at all of the Leg 117 sites are clays and calcite of indeterminate, but not obviously biogenic, origin. This calcite is recorded as "inorganic calcite" in the smear slide analyses but is probably better described as "detrital." This detrital calcite is described by the major compositional modifier "calcitic." The modifier "calcareous" is restricted to describing biogenic calcareous components where component percentages are equivalent. The compositions of biogenic grains can be described by terms that are defined in the following sections.

Table 1. Summary of nomenclature of basic oceanic sediment types.

Minor modifiers	Major modifiers	Main name
Siliciclastic sediments		
1. Composition of minor siliciclastic grains	1. Composition of major siliciclastic grains	1. Texture of terrigenous grains (sand, silt, etc.)
2. Composition of minor biogenic grains	2. Composition of minor biogenic grains	2. Texture of volcaniclastic grains (ash, lapilli, etc.)
Siliceous biogenic sediments		
1. Composition of minor biogenic grains	1. Composition of major biogenic grains	1. Ooze
2. Texture of minor siliciclastic grains	2. Texture of major siliciclastic grains	2. Radiolarite 3. Diatomite 4. Porcellanite 5. Chert
Calcareous biogenic sediments		
1. Composition of minor biogenic grains	1. Composition of major biogenic grains	1. Ooze 2. Chalk 3. Limestone
2. Composition of minor siliciclastic grains	2. Composition of major siliciclastic grains	

Siliceous Biogenic Sediments

Siliceous biogenic sediments are composed of less than 30% clastic grains, less than 30% silt and clay, and greater than 30% siliceous biogenic grains. The main name of a siliceous biogenic sediment describes its degree of consolidation and/or its composition, using the following terms:

1. Ooze: Soft, unconsolidated siliceous biogenic sediment.
2. Radiolarite: Hard, consolidated siliceous biogenic sediment composed predominantly of radiolarians.
3. Diatomite: Hard, consolidated siliceous biogenic sediment composed predominantly of diatoms.

The major and minor modifiers for a siliceous biogenic sediment describe the compositions of the siliceous biogenic grains, as well as the compositions of accessory calcareous biogenic grains and the textures of accessory siliciclastic grains. The compositions of siliceous biogenic grains are described by the terms "radiolarian," "diatomaceous," and "siliceous" if many types are present but none dominates, followed by the suffix "-bearing" if a minor (5% to 10%) amount of the component is present. The compositions of accessory calcareous grains are described by terms that are discussed in the following text; the textures of accessory terrigenous grains are described by the terms discussed in the previous section.

Calcareous Biogenic Sediments

Calcareous biogenic sediments are composed of less than 30% clastic grains, less than 30% siliceous-biogenic grains, and greater than 30% biogenic carbonate grains. The main name of a calcareous biogenic sediment describes its degree of consolidation, using the terms "ooze" (soft, unconsolidated), "chalk" (partially to firmly consolidated), or "limestone" (cemented).

The major and minor modifiers for a calcareous biogenic sediment describe the compositions of calcareous biogenic grains, as well as the compositions of accessory siliceous biogenic grains and the textures of accessory siliciclastic grains.

The compositions of calcareous biogenic grains are described by the terms "foraminifer," "nannofossil," or "calcareous" (for a combination thereof where none dominates), followed by the suffix "-rich" if the grain components are present in abundances of 10% to 25% and by the suffix "-bearing" if the grain components are present in minor (5% to 10%) amounts. The compositions of siliceous biogenic grains and the textures of siliciclastic grains are described by the terms previously discussed.

Special Rock Types

The definitions and nomenclatures of special rock types are not included in the previous section, but their description adheres as closely as possible to conventional ODP terminology. Rock types included in this category include phosphorite and shallow-water limestones (e.g., carbonate grainstones and packstones).

BIOSTRATIGRAPHY

Leg 117 shipboard biostratigraphy was based on planktonic foraminifers, calcareous nannofossils, and radiolarians. Age determinations were based on examination of the core-catcher assemblages and were refined with shore-based studies of intermediate samples.

Correlation of the zonal schemes for these fossil groups with the geomagnetic polarity time scale of Berggren et al. (1985b) is shown in Figure 7 with some modifications. These modifications make the correlation more applicable to the Leg 117 material and take into account studies made after the publication of Berggren et al. (1985b).

The Pliocene/Pleistocene boundary is placed at 1.66 Ma at the first appearance datum (FAD) of *Gephyrocapsa caribbeanica* in accordance with the results of studies of the Italian type section by Sato et al. (in press). The Miocene/Pliocene boundary is placed just above the base of the NN12 Zone in accordance with Berggren et al. (1985b). See the following sections on planktonic foraminifers and radiolarians for additional modifications.

Although shipboard determinations of paleomagnetic reversals were made at a number of sites, we have chosen to use previously published paleomagnetically derived ages in the site chapters (see "Paleomagnetism" section, this chapter). We have, however, used oxygen isotope data from Site 723 (Niitsuma and Oba, unpubl. data) to establish the ages of three late Pleistocene nannofossil events (FAD of *Emiliania huxleyi*, the last appearance datum (LAD) of *Pseudoemiliania lacunosa*, and the top of acme of *Reticulofenestra* sp. A).

Planktonic Foraminifers

A list of stratigraphically useful species events that were recognized in the Leg 117 material is presented in Table 3. Most ages were derived from Berggren et al. (1985b), except for the first occurrences (FOs) of *Sphaeroidinella dehiscens immatura* and *Neogloboquadrina acostaensis*. The *S. dehiscens immatura* appearance datum level (4.8 Ma) of van Gorsel and Troelstra

Table 2. Grain-size categories used for classification of terrigenous sediments (from Wentworth, 1922).

MILLIMETERS		μm	PHI (Ø)	WENTWORTH SIZE CLASS	
			-20		
	4096		-12	Boulder (-8 to -12 Ø)	
	1024		-10		
	256		-8		
				Cobble (-6 to -8 Ø)	GRAVEL
	64		-6		
	16		-4	Pebble (-2 to -6 Ø)	
	4		-2		
	3.36		-1.75		
	2.83		-1.5	Granule	
	2.38		-1.25		
	2.00		-1.0		
	1.68		-0.75		
	1.41		-0.5	Very coarse sand	
	1.19		-0.25		
	1.00		0.0		
	0.84		0.25		
	0.71		0.5	Coarse sand	
	0.59		0.75		
1/2	0.50	500	1.0		
	0.42	420	1.25		
	0.35	350	1.5	Medium sand	SAND
	0.30	300	1.75		
1/4	0.25	250	2.0		
	0.210	210	2.25		
	0.177	177	2.5	Fine sand	
	0.149	149	2.75		
1/8	0.125	125	3.0		
	0.105	105	3.25		
	0.088	88	3.5	Very fine sand	
	0.074	74	3.75		
1/16	0.0625	63	4.0		
	0.053	53	4.25		
	0.044	44	4.5	Coarse silt	
	0.037	37	4.75		
1/32	0.031	31	5.0		
1/64	0.0156	15.6	6.0	Medium silt	
1/128	0.0078	7.8	7.0	Fine silt	
1/256	0.0039	3.9	8.0	Very fine silt	MUD
	0.0020	2.0	9.0		
	0.00098	0.98	10.0	Clay	
	0.00049	0.49	11.0		
	0.00024	0.24	12.0		
	0.00012	0.12	13.0		
	0.00006	0.06	14.0		

(1981) was used, and the *N. acostaensis* FO (8.6 Ma) comes from Barron et al. (1985). These ages are in better correspondence to the calcareous nannofossil and radiolarian datum levels determined from Leg 117 material. During shipboard analysis it appeared that the zonal marker species for published Pleistocene-Pliocene zonal schemes are missing or show a highly scattered occurrence. For instance, the evolutionary series of *Globorotalia tosaensis* to *Globorotalia truncatulinoides* is missing in the upper Pliocene to lower Pleistocene. We approximated this boundary (N21/22) by using the extinction level of *Globigerinoides obliquus extremus* (1.8 Ma). In addition, subdivision of the Pliocene was difficult because of the scarcity of specimens of marker species such as *Globorotalia margaritae* and *Globigerinoides fistulosus*. Because published zonal schemes are difficult if not impossible to apply in this area, we have used the conventional zonation of Blow (1969) as closely as possible.

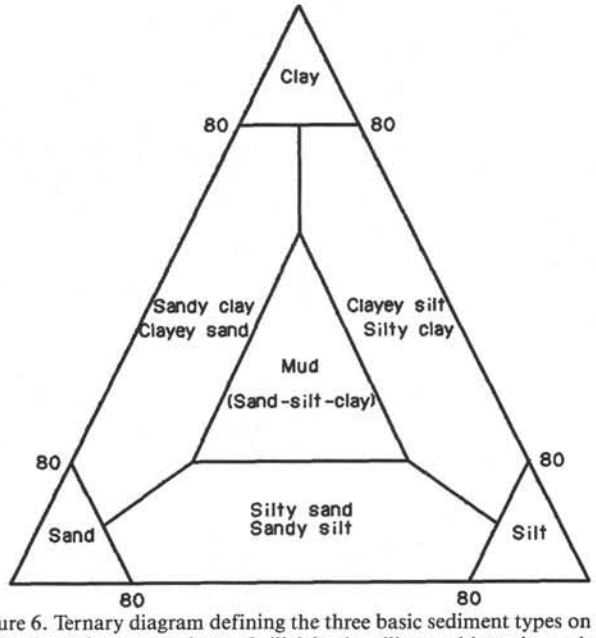

Figure 6. Ternary diagram defining the three basic sediment types on the basis of relative proportions of siliciclastic, siliceous biogenic, and calcareous biogenic grains.

Methods

Sediment samples of approximately 10 cm³ from the core catchers were washed over a 45-μm-mesh sieve to extract sufficient foraminifers. The >125 μm fraction was studied, and the semiquantitative abundance of planktonic foraminiferal species of the total assemblage were estimated as follows:

R = rare (<1%)
F = few (1%–15%)
C = common (15%–30%)
A = abundant (>30%)

In addition, the 63–125-μm fraction was examined for planktonic foraminiferal markers if they were absent in the larger size fraction.

Three classes of foraminiferal preservation were employed:

P = poor (almost all specimens are broken and fragments dominate)
M = moderate (30%–90% of specimens show dissolution)
G = good (>90% of specimens are well preserved and unbroken)

Benthic Foraminifers

Methods

Sediment samples of approximately 10 cm³ were processed for extraction of benthic foraminifers. The sediment samples were wet sieved over a 63-μm sieve, and the residue was dried under an infrared lamp. The benthic foraminifers were then extracted from the >125-μm fraction.

The abundance of benthic foraminifers in 10 cm³ is defined as follows:

R = rare (<10 specimens)
P = poor (10–100 specimens)
C = common (101–500 specimens)
A = abundant (>500 specimens)

Preservation is determined by the degree of fragmentation and abrasion of the benthic tests:

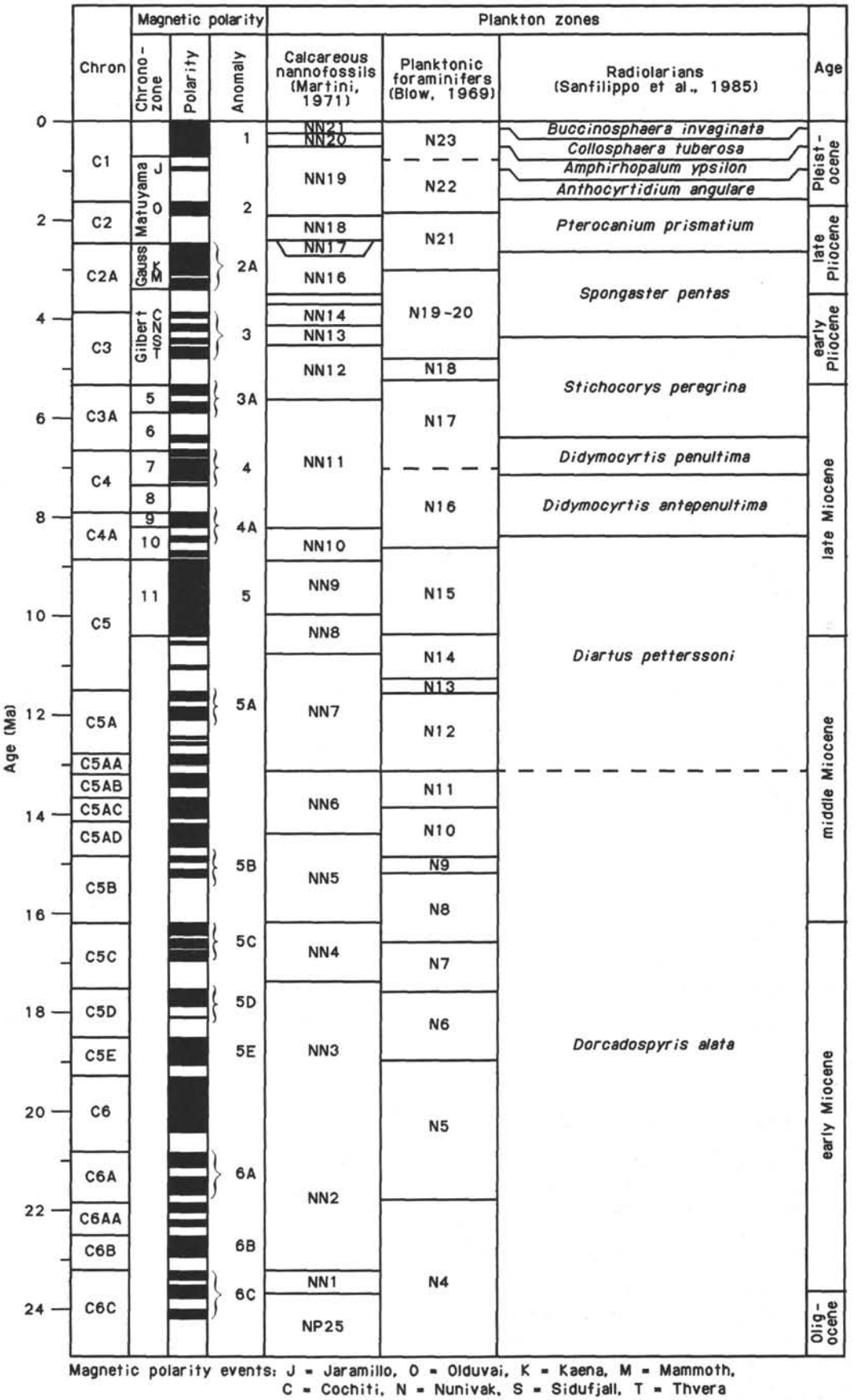

Figure 7. Neogene geochronology modified from Berggren et al. (1985b) for Leg 117.

Table 3. Foraminiferal species events found in Leg 117 material.

Event	Species	Age (Ma)
LO	*Globigerinoides obliquus extremus*	1.8
LO	*Sphaeroidinellopsis* sp.	3.0
Coiling change of S/D *Pulleniatina*		3.8
FO	*Sphaeroidinella dehiscens immatura*	4.8
FO	*Globorotalia tumida tumida*	5.2
FO	*Pulleniatina primalis*	5.8
FO	*Neogloboquadrina acostaensis*	8.6
LO	*Globorotalia mayeri*	10.4
FO	*Globigerinoides nepenthes*	11.3
LO	*Globorotalia fohsi* s.l.	11.5
LO	*Globorotalia peripheronda*	14.6
FO	*Globorotalia peripheroacuta*	14.9
FO	*Orbulina universa*	15.2

Note: FO = first occurrence, LO = last occurrence. Ages are from Berggren et al. (1985b), except for: *Sphaeroidinella dehiscens immatura* (van Gorsel and Troelstra, 1981) and *Neogloboquadrina acostaensis* (Barron et al., 1985).

P = poor (mostly fragments and/or strongly etched specimens)
M = moderate (about 50% of the tests in an assemblage are broken or etched
G = good (most specimens are intact)

Planktonic/benthic ratios were determined in the >125-μm size fraction to reveal dissolution patterns or environmental conditions.

Calcareous Nannofossils

The zonal scheme established by Martini (1971) was employed on this leg. The biohorizons recognized in the Quaternary sequences in the North Atlantic on DSDP Leg 94 by Takayama and Sato (1987) were also used. The nannofossil zonation and the indication of estimated time relations are based on Takayama and Sato (1987) and Berggren et al. (1985b). Nannofossil datums used on Leg 117 are listed in Table 4.

Methods

Age determination made during Leg 117 was based on the study of each core-catcher sample and samples specially selected by the shipboard paleontologists. Shore-based studies are based on slides made from intermediate samples. Nannofossil slides were prepared from unprocessed sample material. These slides were examined under the binocular polarizing microscope at a magnification of 1250× with an oil-immersion objective.

Selective dissolution and overcalcification of calcareous nannofossils are important factors in species identification and species composition in deep-sea sediments, and as such, may have a considerable effect on biostratigraphic results. The overall preservation of the nannofossil assemblage was recorded using one of three letter designations:

G = good (little or no evidence of solution and/or overgrowth
M = moderate (some dissolution and/or overgrowth, but nearly all specimens can be identified
P = poor (dissolution and/or overgrowth on nearly every specimen, and many specimens cannot be identified)

Abundances were estimated semiquantitatively at 1250× magnification and tabulated according to a logarithmic scale as follows:

A = abundant (1 to 10 specimens of a taxon per field of view)
C = common (1 specimen of a taxon per 2 to 10 fields of view)
F = few (1 specimen of a taxon per 11 to 100 fields of view)
R = rare (1 specimen of a taxon per 101 to 1000 fields of view)

Radiolarians

The low-latitude zonations of Nigrini (1971) for the Quaternary and of Riedel and Sanfilippo (1978) and Sanfilippo et al. (1985) for the Tertiary were used on Leg 117 when the zonal markers could be found. *Pterocanium prismatium*, *Spongaster pentas*, and *Spongaster berminghami* are all very rare in Arabian Sea material. Hence, in some cases, other species had to be used to approximate certain zonal boundaries (see individual site chapters). Table 5 lists the radiolarian events used to establish a biochronology for Leg 117. Ages used are from previously published paleomagnetic data for the Indian Ocean (Johnson et al., in press; Johnson and Nigrini, 1985).

Methods

The recorded radiolarian abundance in each sample is based on qualitative examination of strewn slides of sieved acid residues. Consequently, there may be discrepancies between these observations and those in the lithology reports, which were based on smear slide observations. Estimates also reflect, in part, the amount of terrestrial input and nonradiolarian siliceous biota (mainly diatoms). Abundances are recorded as follows:

C = common (100 to 500 specimens in the noncalcareous fraction)
F = few (10 to 100 specimens)
R = rare (3 to 10 specimens)

The preservation of radiolarians in strewn slides is defined as follows:

G = good (no signs of dissolution)
M = moderate (dissolution observed, but minor)
P = poor (strong dissolution effect)

Samples preparation procedures used during this cruise are described in Sanfilippo et al. (1985). All samples were sieved with 63-μm mesh size.

PALEOMAGNETISM

Sampling and Magnetic Measurements

Soft sediments were sampled by pushing plastic cubes of 6 mL volume into the split-core face. For semilithified sediments we used a ceramic knife to cut out samples that were then inserted into the plastic cubes. For lithified sediments we used a diamond-tipped rotary drill to obtain minicores, which were then trimmed to a volume of about 10 mL. We routinely took two samples per 1.5-m core section from suitable (i.e., undisturbed) intervals; this sampling resolution was found to be adequate for resolving the magnetostratigraphy of the generally high accumulation rate sequences encountered on Leg 117. Usually, one of the samples from each section was demagnetized and measured aboard the ship, and the other was kept in its original condition for shore-based measurement.

The natural remanent magnetization (NRM) of the archive halves of cores was measured at 10-cm intervals using the 2G

Table 4. Calcareous nannofossil datums recognized on Leg 117.

Datum	Limit	Species	Age (Ma)	Source of age	Notes
1	T	*Helicosphaera inversa*	0.15	4	North Atlantic data
2	B	*Emiliania huxleyi*	0.19	3	
3	T	*Pseudoemiliania lacunosa*	0.49	3	
4	B	*Helicosphaera inversa*			
5	T	*Reticulofenestra* sp. A (acme)	0.82	3	
6	B	*Gephyrocapsa parallela*	0.89	4	North Atlantic data
7	T	*Gephyrocapsa* (large)	1.10	4	North Atlantic data
8	T	*Helicosphaera sellii*			May be diachronous
9	B	*Gephyrocapsa* (large)	1.36	4	North Atlantic data
10	T	*Calcidiscus macintyrei*	1.45	6	
10	B	*Gephyrocapsa oceanica*	1.57	4	North Atlantic data
	B	*Gephyrocapsa caribbeanica*	1.66	4, 8	North Atlantic age consistent with Italian-type section
	T	*Discoaster brouweri*	1.90	6	
	T	*Discoaster pentaradiatus*	2.40	6	
	T	*Discoaster surculus*	2.40	6	
	T	*Sphenolithus abies*	3.47	6	
	T	*Reticulofenestra pseudoumbilica*	3.50	6	
	B	*Discoaster tamalis*	3.8	6	Equatorial region only
	B	*Discoaster asymmetricus*	4.1	6	
	B	*Ceratolithus rugosus*	4.5	6	
	T	*Discoaster quinqueramus*	5.6	6	May be erroneous age
	B	*Discoaster quinqueramus*	8.2	6	
	T	*Discoaster hamatus*	8.85	6	
	B	*Discoaster hamatus*	10.0	6	
	B	*Catinaster coalitus*	10.8	6	
	B	*Discoaster kugleri*	ca. 13.1	6	
	T	*Sphenolithus heteromorphus*	14.4	6	
	T	*Sphenolithus belemnos*	17.4	6	

Note: T = upper limit and B = lower limit. Sources of ages are: 3 = oxygen isotope data for Site 723 (N. Niitsuma, unpubl. data); 4 = Takayama and Sato, 1987; 6 = Berggren et al., 1985b; and 8 = Sato et al., in press.

Enterprises pass-through cryogenic magnetometer; measurements were usually made after alternating field (AF) demagnetization at 5 or 9 mT with the pass-through demagnetizer. Pass-through NRM measurements were usually confined to APC cores; measurements obtained from XCB recovery were typically much more scattered. The NRM of discrete specimens was measured using the MINISPIN fluxgate spinner magnetometer and the Schonstedt AF demagnetizer. Where possible (depending on time constraints) one sample per core was subjected to stepwise AF demagnetization in order to select a suitable field for blanket demagnetization of the remaining samples from that core.

Most of the samples measured aboard ship were remeasured onshore with a ScT cryogenic magnetometer involving application of a higher peak AF (usually 15 mT) for demagnetization. Because the shore-based remeasurement generally confirmed the shipboard results, most of the magnetic polarity zone boundaries cited in the site chapters are those that were determined aboard ship. Resolution of some boundary horizons was, however, improved by the shore-based reanalysis. The volume magnetic susceptibility of whole cores was measured (usually at 5–10-cm intervals) using the Bartington Instruments MS1C sensor; the instrument was calibrated by calculating the volume susceptibility of a 30-cm length of core liner packed with MnO_2 as a standard.

Geomagnetic Polarity Time Scale

We use the geomagnetic polarity time scale (GPTS) of Berggren et al. (1985a). Our choice of chron nomenclature follows the marine magnetic anomaly-based system described in Cox (1983) with the addition of the prefix *C* (correlative). For convenience, in referring to chrons we include the traditional terminology used in chronostratigraphic unit in parentheses: e.g., chron C1N (Bruhnes chronozone) and chron C5N (chronozone 11). Using the depth and the age of our paleomagnetic polarity zone boundaries, we calculated interpolated ages for biostratigraphic datum levels. The paleomagnetic records from some sites, however, are incomplete, making accurate interpolation difficult. We could not find good records of relatively short polarity "events," such as C1r-1 (Jaramillo subchronozone) and C2N (Olduvai subchronozone) at the Owen Ridge sites and at Site 728 on the Oman margin. Furthermore, uncertainty exists as to whether the sedimentation rate was constant enough during a polarity chron. Therefore, we are reluctant, at this time, to accept the interpolated ages as reliable age estimates of biostratigraphic datums.

INTERHOLE AND INTERSITE CORRELATIONS

Because the recovery of several complete Neogene sequences was a primary objective of Leg 117 drilling, the ability to correlate between holes so that complete composite sequences could be constructed for a given site was of critical importance. As most of the sites are represented by two to three holes, the potential for constructing complete sequences is good. We applied two methods of correlation: visual comparison of the core photographs and correlation using whole-core magnetic susceptibility measurements.

For many of the sites, the dominant lithology consists of alternating layers of light, carbonate-rich intervals and darker, clay-rich intervals. Interhole comparison of core photographs indicated that these sedimentary layers could be visibly correlated between holes based on their color and thickness characteristics. Using the core photographs, the sedimentary layers could be correlated between holes to within 5–10 cm. For the Oman margin sites, and particularly for the Owen Ridge sites, several distinct and traceable layers were identified. Owen Ridge Hole 721A was the first hole for which these layers were observed and described, with the notation OR-a_0, a_1, . . ., a_n and OR-b_1, b_2, . . ., b_n. The OR-*a* indicates that the marker layer was first observed in Core 117-721A-1H, and the OR-*b* refers to layers observed in Core 117-721A-2H. The numbered subscripts identify the layer's sequence in a given core. Intersite correlation of these

Table 5. List of radiolarian events, their placement in the zonal scheme of Sanfilippo et al. (1985), and correlation with previously published paleomagnetically derived ages.

Radiolarian zone	Radiolarian event	Indian Ocean age (Ma)	Source of age	Notes
Buccinosphaera invaginata	**B *Buccinosphaera invaginata***	—		
Collosphaera tuberosa	T *Stylatractus universus*	0.37–0.47	1	
	B *Collosphaera tuberosa*	0.40–0.59	1	
Amphirhopalum ypsilon	T *Anthocyrtidium nosicaae*	0.66–0.76	1	
	B *Pterocorys hertwigii*	0.76–0.84	1	
	T *Anthocyrtidium angulare*	0.94–1.04	1	
Anthocyrtidium angulare	B *Lamprocyrtis nigriniae*	1.02–1.07	1	Possibly a diachronous event
	T *Lamprocyrtis neoheteroporos*	1.09–1.13	1	
	T *Pterocanium prismatium*	1.52–1.56	1	Rare in Leg 117 material
	B *Anthocyrtidium angulare*	1.52–1.64	1	
Pterocanium prismatium	B *Theocalyptra davisiana*	2.42–2.44	1	
	B *Lamprocyrtis neoheteroporos*	2.51–2.53	1	
	T *Stichocorys peregrina*	2.62–2.64	1	
	T *Phormostichoartus fistula*	3.26–3.28	1	
	T *Lychnodictyum audax*	3.33–3.35	1	
Spongaster pentas	T *Phormostichoartus doliolum*	3.53–3.55	1	
	B *Amphirhopalum ypsilon*	3.77–3.79	1	
	T *Spongaster pentas*	3.74–3.82	1	Not found in Leg 117 material
	B *Spongaster tetras tetras*	3.83–3.85	1	
	T *Spongaster berminghami*	3.85–3.87	1	Rare in Leg 117 material; possibly a diachronous event
	Spongaster berminghami* → *Spongaster pentas	4.3–4.4	2	Rate in Leg 117 material; possibly a diachronous event
	B *Spongaster pentas*	4.2–4.3	2	Rare in Leg 117 material; a diachronous event
	T *Solenosphaera omnitubus*	4.7–4.8	2	
	T *Spongodiscus ambus*	—		
	T *Botryostrobus bramlettei*	4.9–5.0	2	Not reliable in Leg 117 material
	T *Stichocorys delmontensis*	—		
Stichocorys peregrina	T *Siphostichartus corona*	5.0–5.1	2	
	T *Acrobotrys tritubus*	5.3–5.4	2	
	T *Stichocorys johnsoni*	5.7–5.8	2	*Eucyrtidium* cf. *diaphanes*
	B Spongodiscus ambus	—		
	Stichocorys delmontensis* → *Stichocorys peregrina	6.1–6.7	2	Possibly a diachronous event
Didymocyrtis penultima	T *Calocycletta caepa*	6.2–6.6	2	Age in west Pacific; possibly a diachronous event
	B *Solenosphaera omnitubus*	6.3–6.5	2	
	T *Diartus hughesi*	7.1–7.2	2	
	B *Stichocorys peregrina*	—		
	T *Dictyocoryne ontongensis*	—		
Didymocyrtis antepenultima	B *Acrobotrys tritubus*	7.7–7.78	2	Diachronous event
	T *Botryostrobus miralestensis*	8.1–8.2	2	Possibly a diachronous event
	T *Didymocyrtis laticonus*	—		
	T *Diartus pettersoni*	8.1–8.2	2	Possibly a diachronous event
	Diartus pettersoni* → *Diartus hughesi	8.3–8.5	2	Possibly a diachronous event
	B *Spongaster berminghami*	7.9–8.0	2	Rare in Leg 117 material; possibly a diachronous event
	T *Stichocorys wolffii*	8.1–8.2	2	Age in west Pacific
Diartus pettersoni	B *Botryostrobus bramlettei*	8.8–9.0	2	
	B *Diartus hughesi*	8.7–8.8	2	Diachronous event
	T *Cyrtocapsella japonica*	10.0–10.3	2	Possibly a diachronous event
	T *Lithopera thornburgi*	—		
	T *Cyrtocapsella cornuta*	11.6–11.9	2	

Note: T = upper morphotypic, B = lower morphotypic limit, and → = evolutionary transition. Events shown in bold face define zonal boundaries. Sources of ages are: 1 = Johnson et al., in press, and 2 = Johnson and Nigrini, 1985.

lithologic marker layers applies only to the Owen Ridge Sites 721, 722, and 731. The depths of the correlative horizons are listed in the respective site chapters.

Hole 723A was the first hole for which lithologic marker layers were identified for the Oman margin. As with the Owen Ridge sites, the marker layers were labeled OM-a_1, a_2, . . ., a_n and OM-b_1, b_2, . . ., b_n, with the *a* indicating that the layer occurs in Core 117-723A-1H and the numbered subscript identifying its sequence in that core.

These interhole correlations were confirmed using whole-core magnetic susceptibility measurements. The magnetic susceptibility of whole-core sections was measured at 5- to 10-cm intervals for all APC-recovered core material and most XCB- and RCB-recovered material. To the first order, downcore variations in magnetic susceptibility record reflect fluctuations in the concentration of magnetic materials, which are dominantly the ferrimagnetic minerals of the magnetite-titanomagnetite series for most marine sediments. In general, the darker, clay-rich intervals are identified by higher values of magnetic susceptibility. Compared to the lithologic datums, the susceptibility variations offer considerably more detail and character with which to construct correlations, and the data are quantitative (Fig. 8). By combining the lithologic and magnetic susceptibility correlation datums, it is possible to cross-validate proposed lithologic cor-

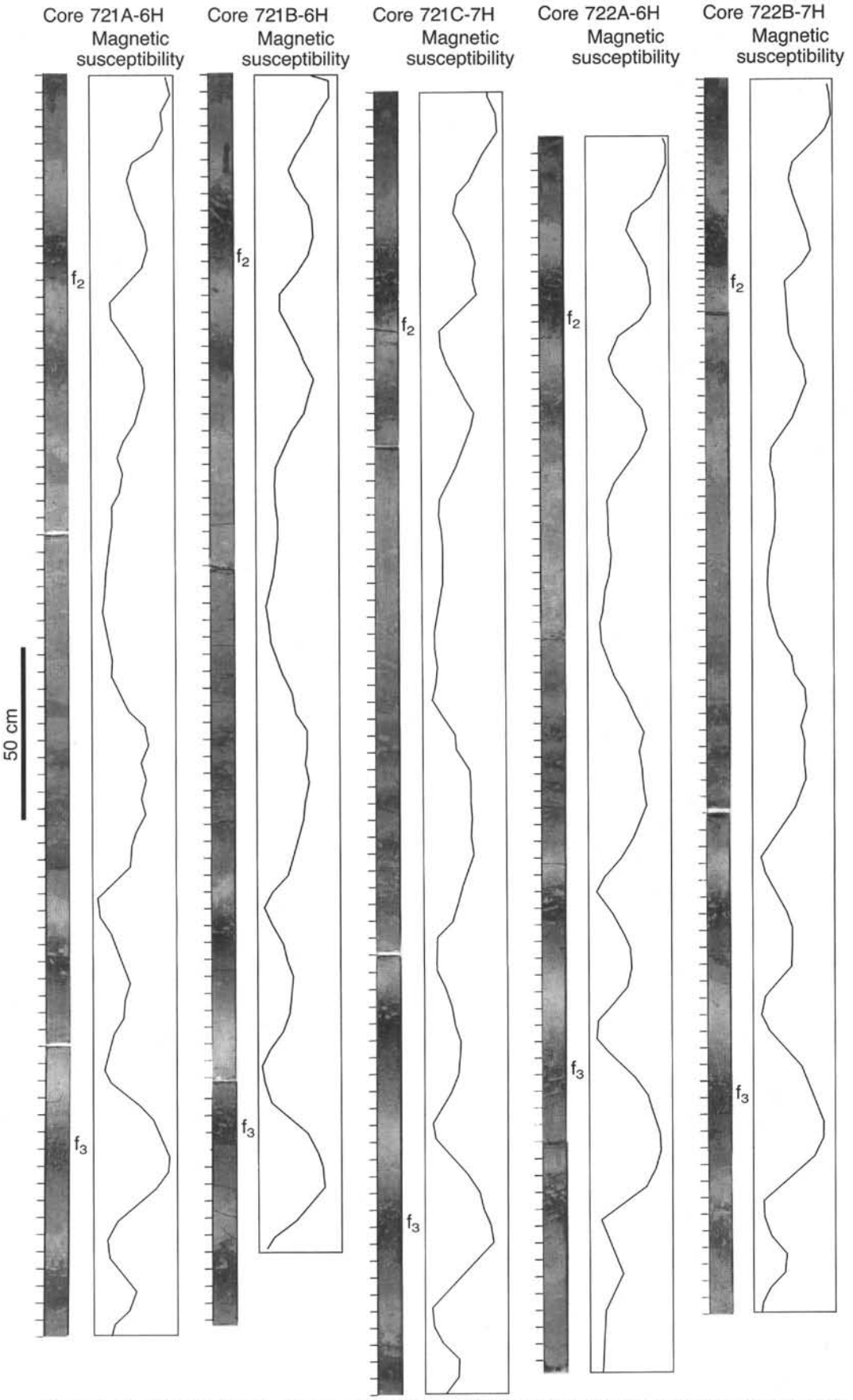

Figure 8. Example of sediment color and magnetic susceptibility measurements correlation used between hole and sites. See text for detailed explanation.

relations to obtain definitive correlation datums that are both detailed and accurate. For the Owen Ridge sites, the correlation accuracy is typically within ± 5 cm. The accuracy of the Oman margin correlations are comparable for the uppermost APC cores; however, correlations were typically not possible beyond ~ 50 mbsf because of the adverse effect of gas-expansion disturbances on both lithologic and magnetic datums.

Correlation datums given in the "Interhole and Intersite Correlations" sections of the "Site 721–724, 727, and 728" chapters are based on concordant lithologic and magnetic datums only. The intended application of these datums is to provide a series of connection points from which accurate interhole correlations can be made. The lithologic and magnetic susceptibility data from Owen Ridge Sites 721, 722, and 731 indicate that up to 1 to 2 m can be missing at APC core breaks; thus, the interhole correlation datums are necessary to compose complete sections around core breaks and voids (Fig. 9). For the ridge sites, the correlation datums allow a complete composite section to be constructed from the upper Pliocene upward. The margin sites have a wider range of sedimentation rates, but complete sections for some sites can be constructed for the upper Pliocene upward (Sites 727 and 728) and for the upper Pleistocene (Sites 723 and 724).

Intersite Correlations

Intersite correlations for the Owen Ridge sites and the Oman Margin sites are presented in the "Background and Objectives, Owen Ridge" and the "Background and Objectives, Oman Margin" chapters (this volume). As with the interhole correlations, the datums given in these chapters are based on concordant lithologic and magnetic susceptibility correlations. These correlations are generally accurate to within 10 cm. Between the Owen Ridge Sites 721, 722, and 731, intersite correlations are possible from the upper Pliocene upward. An example of correlation between cores of the three Owen Ridge sites is shown in Figure 8. Correlations between Owen margin Sites 727 and 728 are possible down to the upper Pliocene; correlations between margin Sites 723 and 724 are possible down to the upper Pleistocene only.

The combination of excellent Leg 117 sediment recovery and firm stratigraphic control allows the construction of complete composite sequences. Correlation datums provided in the site chapters have been confirmed using both lithologic and magnetic susceptibility datums. The detail of the interhole and intersite correlations is among the best reported for any drilled marine sequence recovered to date. Although the principal application of the correlation datums is to provide a means for composing complete sequences, they also serve to maximize sampling economy and diffuse future sampling intensity at any one hole.

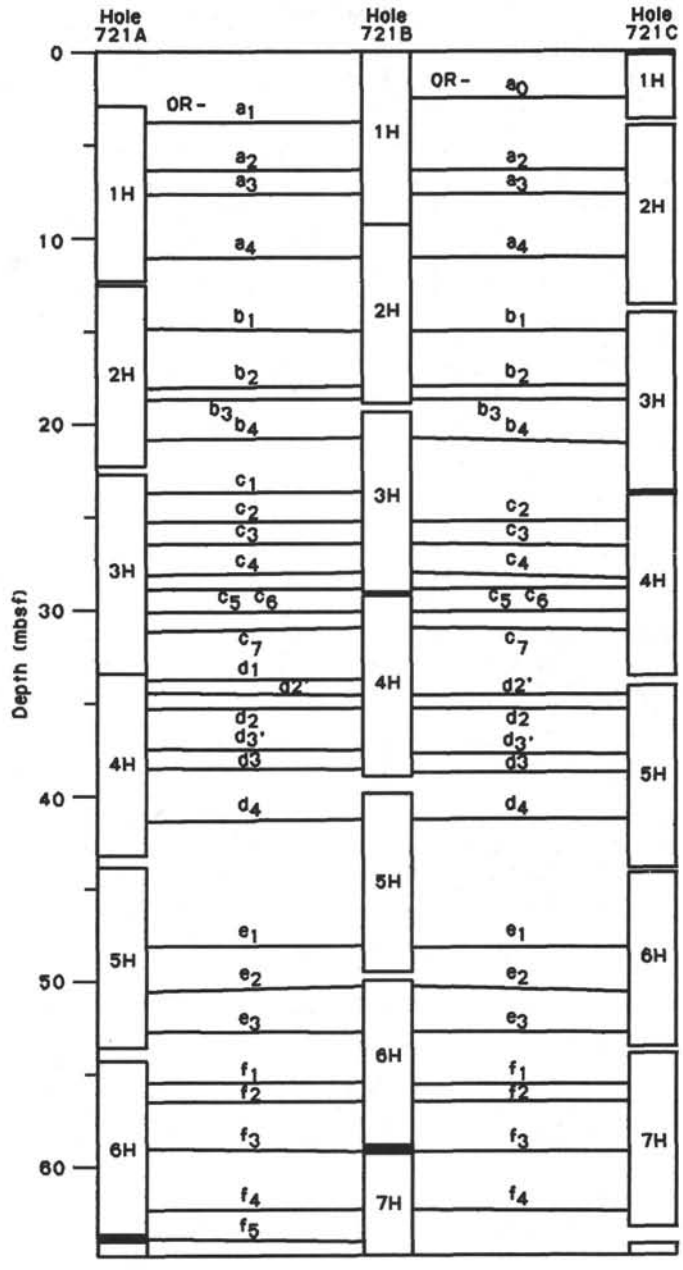

Figure 9. Correlation of sedimentary layers based on color and thickness (see text) for Holes 721A, -B, and -C, Cores 1–7.

PHYSICAL PROPERTIES

A thorough discussion of the equipment, methods, errors, and correction factors associated with the measurement of physical properties was presented by Boyce (1973, 1976). Only a brief review of the methods used on Leg 117 is presented here.

Gamma Ray Attenuation Porosity Evaluator (GRAPE)

The gamma ray attenuation porosity evaluator (GRAPE) consists of a drive device to move a gamma-ray source (^{133}Ba) and a shielded scintillation detector along the length of whole-round core sections. The attenuation of the gamma rays through the cores is directly correlated with the material's mass density, producing a continuous log of wet-bulk density. Details of the theory and operation of the GRAPE can be found in Boyce (1973, 1976). The GRAPE system was calibrated periodically with an aluminum standard; an error of 1.5% is estimated by Boyce (1976). The GRAPE density values were strongly affected by the degree to which the core material filled the core liners. On Leg 117 all coherent APC and XCB core sections more than 80 cm in length were run through the GRAPE.

In order to process the large volume of sediment recovered during Leg 117 it was necessary to modify the GRAPE software to increase the carriage speed by a factor of three to a rate of 0.76 cm/s. The duration of each gamma-ray count was not changed from the original 2-s count period followed by a 0.33 s break time between counts. Given this count interval and the new carriage speed, each gamma-ray count sampled a 1.5-cm-wide interval of core.

Two-minute GRAPE measurements on discrete samples were not routinely run on unlithified samples because of the large volume of sediment processed in the continuous mode. This technique, as described by Boyce (1976), was used, however, on samples of indurated sandstone.

Compressional-Wave Velocity

Compressional-wave velocities were measured through sediments and sedimentary rocks using two devices and techniques: (1) IOS Compressional-Wave Core Logger (*P*-wave logger), a continuous whole-core logging device (Schultheiss et al., 1988), and (2) Hamilton Frame Velocimeter (Boyce, 1973). All velocity measurements were made at atmospheric pressure.

The *P*-wave logger (PWL) measures the compressional-wave velocity perpendicular to the axis of the core at 2-mm intervals as the core is passed between two 500-kHz PZT4 piezoelectric compression-mode ultrasonic transponders. Variations in liner diameter are measured by displacement transducers, linear 1-K potentiometers with 12.5 mm of travel, mounted on the transducer blocks and coupled to the ultrasonic transponders. This apparatus provides good quality data only on undistrubed cores that completely fill the liner. Thus, it is best suited to APC cores, although reliable data can be obtained from suitable XCB cores. All cores were allowed to equilibrate to near room temperature, and corrections of 2.4 m/s/°C were applied to sections at temperatures other than 20°C.

The Hamilton Frame Velocimeter, linked to a Tektronix 5110 oscilloscope and Tektronix TM5006 counter/timer, was used to measure compressional-wave velocities at 500 kHz in discrete samples of sediment and sedimentary rock from all recovered cores that were sufficiently indurated to allow preparation of a suitable sample. See Boyce (1976) for details of operation of the Hamilton Frame Velocimeter.

The velocity measurements were primarily taken perpendicular to bedding, but where the sample conditions allowed, cube samples were cut and measurements were also taken parallel to bedding. Velocity anisotropies were calculated following the expressions of Carlson and Christensen (1979), where anisotropy is given as the ratio of velocity difference to the mean velocity, expressed as a percentage:

$$A = 200\ (V_n - V_v)/(V_n + V_v),$$

where V_n = velocity measured parallel to bedding and V_v = velocity measured perpendicular to bedding.

In a few cases, samples displayed negative velocity anisotropies (more rapid transmission in the direction perpendicular to bedding than parallel to bedding). These data were considered erroneous and were not included in the calculation of "average values."

Index Properties

Index properties (wet-bulk density, grain density, wet water content, and porosity) were routinely calculated from measurements of wet and dry weights and volumes. Samples of approximately 10 cm^3 were taken from every second core section or as sample quality permitted and placed in preweighed and numbered aluminum beakers. Sample weights were obtained to an accuracy of 0.01 g on a Scitech electronic balance. Sample volumes were measured with the shipboard Quantachrome Penta-Pycnometer, a helium-displacement pycnometer. The samples were oven dried at 105°C for 24 hr and allowed to cool in a desiccator prior to dry weight and volume determination. A salt correction (Hamilton, 1971) was applied to the density and porosity computations.

Vane Shear Strength

Shear-strength measurements were made using a Wykeham Farrance Laboratory vane apparatus according to the specifications of Boyce (1977). Approximately one measurement per core was taken on recovery of relatively undisturbed clay-rich sediments. All vanes were inserted parallel to bedding. Measurements were discontinued where cracking of the sediment was observed, indicating failure by fracture rather than by shear. Shear-strength measurements were not made on sediments that were disrupted by gas-induced expansion.

Thermal Conductivity

Thermal-conductivity measurements were made using the THERMCON-85 thermal conductivity instrument supplied to ODP by Woods Hole Oceanographic Institution. The needle probe technique employed by the THERMCON-85, developed by Von Herzen and Maxwell (1959), is described along with the operating procedures for the THERMCON by Pelletier and Von Herzen (unpubl. data). Measurements were taken on every other section of sediment from recovered core that was undisturbed and soft enough to allow insertion of the needle probes. All cores were allowed to equilibrate to room temperature for 3 hr or until temperature drift at the time of measurement was not greater than 0.04°C/min.

Downhole Temperature Measurements

All Leg 117 downhole temperature measurements were obtained using the combination water sampler-temperature-pressure (WSTP) tool first used on Leg 110 (Barnes, 1988). No multichannel data recorder was available for Leg 117; consequently, no fluid-pressure measurements were made. A single-channel data recorder (Yokota et al., 1980) was used to record temperatures measured by a thermistor, placed in a slightly tapered probe that extends 7.8 cm beyond a larger 6.03-cm-diameter filter probe. The larger filter probe extends 109 cm beyond the 8.89-cm diameter of the inner core barrel-WSTP tool assembly. A 10.16-cm-long cylindrical filter element at the bottom of the filter probe is approximately 12 to 22 cm above the thermistor. The lower 2.5 cm of the thermistor probe above the thermistor position has a uniform diameter of 1.27 cm (see Fig. 10).

The Leg 117 filter probe/thermistor probe assembly is an improved version of the probe design that has been used since DSDP Leg 69. The improvements include a larger filter surface area for increased pore fluid recovery, a larger diameter filter probe constructed of high-strength stainless steel, and a thermistor probe strengthened by tapering the upper section to a larger diameter than the previously uniform 1.27 cm. The new probe is 2.6 times stronger than the old probe, eliminating the need to use shortened probe lengths in stiff sediments. Probes shorter than 10.9 cm compromise the ability to obtain uncontaminated fluid samples and undisturbed temperature readings. The time constant of the thermistor probe is 2 to 3 min (Becker et al., 1983).

The Uyeda temperature recorder (Yokota et al., 1980) digitizes and stores up to 128 resistance values of a single thermistor in solid-state memory. The recording interval is 1 or 2 min. A 1-min recording interval was used during Leg 117. Resistance values are converted to temperature by the data reduction program, using the calibration curve for the thermistor in use. The nominal resolution is about 0.01° to 0.02°K over the temperature range of interest.

ORGANIC GEOCHEMISTRY

The following instrumentation and procedures were used on Leg 117 in order to determine the quantity and quality of sedimentary organic matter, to test the reproducibility of the Rock-Eval II apparatus, to measure the concentrations of hydrocarbon gases, and to calculate the ratio of diunsaturated and triunsaturated C_{37} alkenones (U^k_{37} index).

Inorganic and Organic Carbon

The mode of occurrence of carbon was determined by two CO_2 coulometers (Coulometrics Model 5011). Carbon from or-

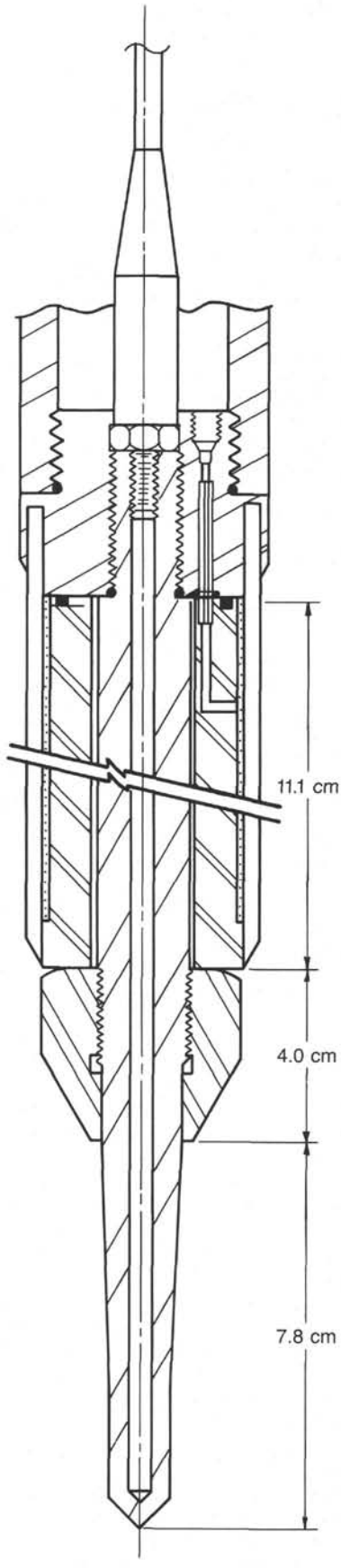

Figure 10. Cross section of the new WSTP tool filter probe/thermistor probe assembly.

ganic and inorganic sources was converted to CO_2, with the gas passed through a coulometer where it was quantitatively absorbed, reacting with monoethanolamine to form a titratable acid that causes a color indicator to change. The color change was monitored electronically. As the transmittance increased, the titration current was activated to stoichiometrically generate base at a rate proportional to the transmittance. The titration current was continually measured and integrated to provide a measure of CO_2.

The CO_2 coulometer serves as the detector for the Carbonate Carbon Apparatus (Coulometrics Model 5030) and the Total Carbon Apparatus (Coulometrics Model 5020). In the Carbonate Carbon Apparatus, CO_2 was generated by treatment of the sediment with HCl and gentle heating; the evolved CO_2 was transferred to the coulometer by a helium stream. Sample size varied between 15 and 75 mg of sediment. In the Total Carbon Apparatus, CO_2 was produced by the combustion of sediment at about 990°C in an oxygen atmosphere. Sample sizes ranged between 20 and 60 mg of sediment. Organic carbon was determined by the difference between total carbon and carbonate carbon. Pure calcite was used as an internal standard.

Type of Organic Matter

The character and maturity of organic matter was evaluated by means of the Delsi Rock-Eval II pyrolysis apparatus, following the process described by Espitalié et al. (1977). The Rock-Eval II is equipped with a TOC module, capable of measuring total organic carbon concentrations. However, these shipboard organic carbon values proved to be unreliable. The pyrolysis technique involved a graduated temperature program that first released volatile hydrocarbons at 300°C for 3 min and then released hydrocarbons from the thermal cracking of kerogen as the temperature increased by 25°C/min from 300° to 550°C. The total volatile (S1) and total pyrolytic (S2) hydrocarbons were measured by a flame ionization detector and are reported in mg of hydrocarbon per gram of sediment. The maximum temperature (T_{max}) value obtained corresponds to the temperature at which the kerogen yielded the maximum amount of hydrocarbons during the programmed pyrolysis. During the pyrolysis cycle, CO_2 produced from organic matter from 300° to 390°C was trapped by a molecular sieve and subsequently analyzed by a thermal conductivity detector (S3). The units of S3 are mg of CO_2 per gram of sediment. Sample size was typically 100 mg. The Rock-Eval parameters are used to calculate Production Index (PI) = S2/(S1 + S2), Petroleum Potential or Pyrolyzed Carbon (PC) = 0.8(S1 + S2), Hydrogen Index (HI) = 100(S2)/TOC, and Oxygen Index (OI) = 100(S3/TOC). Only the latter two indices are reported in the site chapter tables. Results of samples with organic carbon values below 0.25% are not reported here.

Standarization of the Rock Eval was done with the IFP "55000" standard, having the following pyrolytic characteristics: S2 = 8.62 ± 2.5%; S3 = 1.00 ± 8%; T_{max} = 419 ± 1°C, and TOC = 2.86 ± 3.5%. Calibration was checked with the internal "KFA" standard of the Institute of Petroleum and Organic Geochemistry (KFA, Jülich, FRG) with the following pyrolytic characteristics: S2 = 10.54, S3 = 0.54, T_{max} = 424°C, and TOC = 2.16%. Generally, the results of the internal standard were satisfactory. A test of the accuracy and precision of the standard (Table 6) showed that the variation of the S2 and S3 values is minor within one batch, but that the variations in the S2/S3 ratio and between different batches cannot be ignored, especially when one is dealing with samples characterized by low S3 values. Over 400 samples were analyzed with the Rock-Eval apparatus during Leg 117, and a surprisingly good correlation was observed between the organic carbon content (determined by difference) and the S2/S3 ratio. Within one

Table 6. Rock-Eval pyrolysis characteristics of the "KEA" internal standard. Two batches were run on different days, each after standarization with the "55000" standard.

T_{max}	S_2	S_3	S_2/S_3
Batch 1			
430	11.07	0.35	31.62
425	11.41	0.41	27.82
432	10.85	0.45	24.11
429	11.88	0.49	24.24
428	11.98	0.38	31.52
429	11.46	0.52	22.03
Batch 2			
416	13.00	0.51	25.49
420	12.64	0.51	24.78
420	12.87	0.51	25.23
418	12.27	0.53	23.33
421	12.27	0.46	26.89
418	12.99	0.48	27.06
419	12.71	0.54	23.53
420	12.78	0.42	30.42
421	11.75	0.49	23.97

sample batch, correlation coefficients of over 0.9 were common. This seemed to be suspicious and, therefore, several experiments were carried out to be sure that we were not dealing with an artifact. The "55000" standard, the "KFA" standard, and a sample with a high S3 value were diluted with 25%, 50%, and 75% pure calcite, as well as with organic-matter-free sand. The S2 values showed the suspected proportional decrease, but the S3 values showed a decrease that was not proportional to the percentage of dilution, giving rise to lower S2/S3 ratios. The S2/S3 ratio of the diluted sample batch has a high correlation with the organic carbon content. Therefore, all the measured S3 values as well as the calculated oxygen indices as reported in the pertinent tables should be interpreted with extreme caution. After changing the molecular sieve, the same experiments were carried out once more with satisfactory results, i.e., the S2/S3 ratio remained constant. However, S3 values that dropped below 0.5 the analytical error of the Rock-Eval apparatus gave rise to unreliable results.

Hydrocarbon Gases

The compositions and concentrations of hydrocarbon gases in gas pockets, as well as those extracted from sediments, were measured on a Hach-Carle AGC Series 100 gas chromatograph (Model 211). Quantitative analyses of hydrocarbon gases, extracted from sediments, were performed with the so-called headspace procedure. A measured volume of sediment, usually 5 cm^3, was placed in a 22-cm^3 glass vial, sealed with a crimp cap. The vial was heated at 70°C for 45 min, and a portion of the gas inside the vial was analyzed by gas chromatography. A calibrated plunger was used to obtain a measured volume of sediment. The gas chromatograph was attached to a Hewlett-Packard Model 3393A Integrator, which permitted the single measurement of gas concentrations over six orders of magnitude after appropriate calibration. The HC instrument is designed to measure accurately and rapidly the concentrations of methane, ethane, and propane within 5 min. Sporadically, the HC was run for 16 min in order to determine qualitatively the presence of isobutane and butane. The HC is equipped with an 1.0 mL sample loop with column backflush and a column (1.8 m in length and 0.32-cm inner diameter) packed with 80% Poropak N + 20% Poropak Q (80/100 mesh) and flame ionization detector. The sample is run isothermally at 90°C with helium as carrier gas at 60 psi head pressure.

Lipid Analyses

Extraction

Wet sediment samples of approximately 10 cm^3 were lyophilized, homogenized in a mortar, and ultrasonically extracted for 10 min with approximately 20 mL dichloromethane. Following extraction, the sample was centrifuged, and the clear supernatant solution was pipetted off. The extraction was repeated with an additional 10 mL. The combined extract was evaporated by rotary evaporation and taken up in hexane. The hexane-soluble lipids were then transferred into a screw-top vial and concentrated under a gentle stream of nitrogen. No preseparation into different classes of compounds was made. Prior to use, all glassware was thoroughly washed with a soap solution, followed by three water rinses, two rinses with deionized water, and two rinses with dichloromethane. A blank procedure was run to check for contamination in the lab, but no major contaminations were observed.

Gas Chromatography

Gas chromatography was carried out with a Hewlett-Packard Model 5890A Gas Chromatograph equipped with a fused silica capillary column (25 m in length and 0.20-mm inner diameter), split injection, and flame ionization detection. Helium was used as carrier gas with 30 psi head pressure. Injector temperature was 250°C, and a multiramp temperature program (initial = 40°C for 3 min; 10°C/min to 220°C; 220°C for 1 min; 4°C/min to 300°C; isothermal = 15 min) was applied in order to obtain a separation of the long-chain alkenones. The detector temperature was kept at 300°C. Typically, 2 μL of hexane solution was injected with a 10-μL syringe.

Identification of Long-Chain Alkenones

The identification of diunsaturated and triunsaturated C_{37} alkenones in sediment extracts was established by coinjection with an extract from *Emiliania huxleyi*, available aboard ship since Leg 108 (Fig. 11). Calculation of the U^k_{37} ratio was made by peak height and hand-drawn base line.

Shipboard Contamination

Possible organic contaminants aboard *JOIDES Resolution* have been reported by Dunham (1987) and Kvenvolden and McDonald (1986). However, these authors overlooked the most obvious and most important contaminant, the acetone used on the catwalk to glue end caps to the core liner. The contamination of acetone in C_2–C_8 hydrocarbon studies was reported by Schaefer et al. (1983) and Schaefer and Leythaeuser (1984). The contamination was found to be more pronounced at the ends of a core section then in the middle. Fifteen milliliters of acetone, the approximate volume used to seal an end cap, was evaporated to dryness and taken up in 1 mL hexane. The gas chromatogram produced is shown in Figure 12. An unresolved complex mixture of high relative intensity is present and should be taken into consideration when observed in extracts from sediments. To minimize this contamination, organic geochemical samples should be taken in the middle of a section.

INORGANIC GEOCHEMISTRY

Interstitial-water samples were collected either by squeezing 5- or 10-cm whole-round sediment samples or with the Barnes *in-situ* pore-water sampler. Shipboard analyses included determinations of pH, alkalinity, salinity, magnesium, calcium, sulfate, chloride, phosphate, ammonia, and silica. Dissolved or-

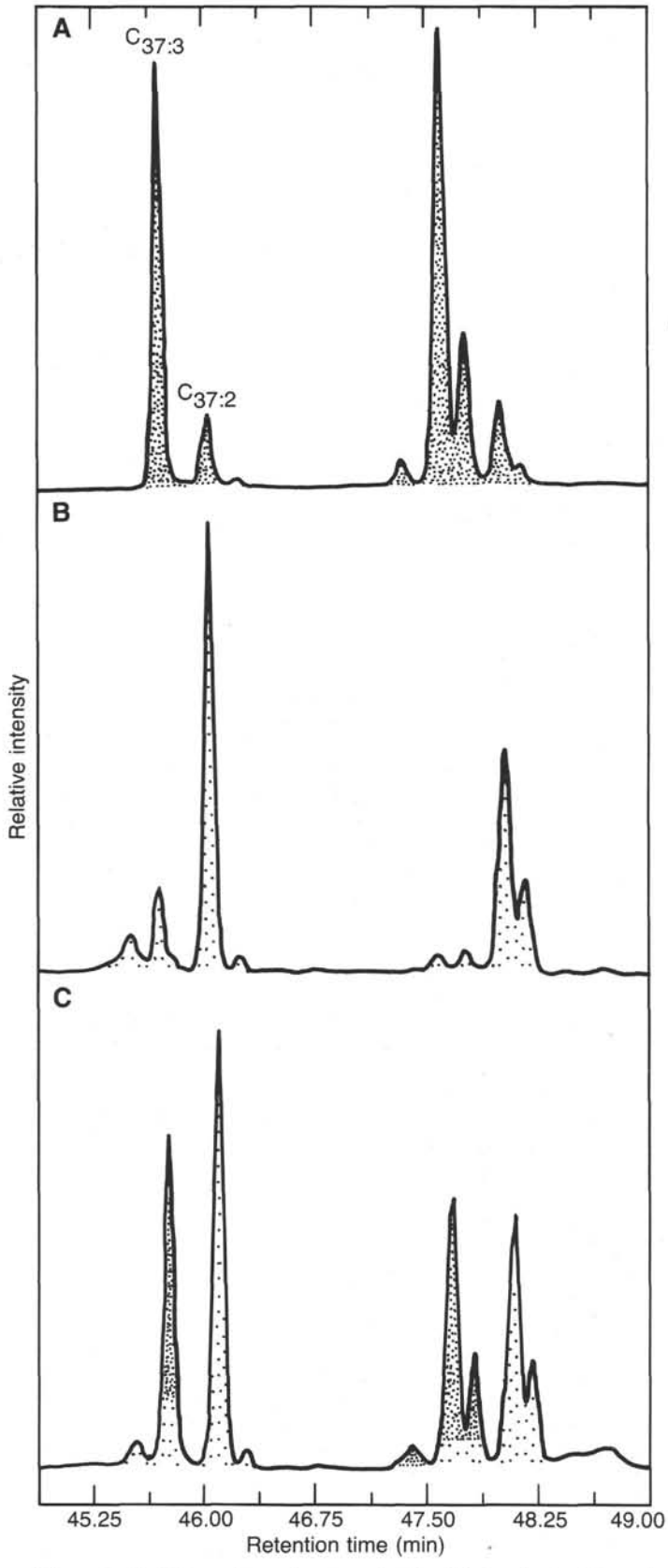

Figure 11. Partial gas chromatograms showing (A) standard mixture of long-chain unsaturated ketones extracted from *Emiliania huxleyi*, (B) extract from Hole 723B sediment sample, and (C) coinjection of A and B.

ganic carbon was measured at the Oman margin sites and at Site 731 on the Owen Ridge. Water was obtained by squeezing the samples in a stainless-steel press at a maximum pressure of 40,000 psi, collected in plastic syringes, and filtered through disposable 0.45-μm Gelman membrane filters. The primary standard used for the interstitial-water analyses was IAPSO standard seawater.

The pH and alkalinity were determined using a Metrohm 605 autotitrator pH meter coupled to a Hewlett-Packard microcomputer that automatically controlled the 0.1 M HCl titer and calculated the Gran function to determine alkalinity. The pH meter was calibrated with NBS standard buffer solutions with pH values of 4.01, 6.86, and 7.41. For alkalinity standardization, 2 to 5 mL of IAPSO standard seawater was used for each determination (see Table 7 for estimates of the relative precision of this method and the others described here).

Salinity values were determined from the refractive index of the water sample measured by a Reichert optical refractometer calibrated in g/kg units. The error on this method was approximately ± 0.2 g/kg.

Sulfate concentrations were measured using the Dionex 2120i ion chromatograph, following dilution of 0.2 cm^3 of the sample to 100 cm^3 with deionized, low-conductivity water. Standardization was achieved using IAPSO standard seawater and artificial standards prepared by J. M. Gieskes.

Chloride, magnesium, and calcium concentrations were analyzed by microtitration using a Metrohm Dosimat titrator. Calcium was determined by the miniversion method of Tsunogai et al. (1968). Magnesium determinations were made after titrating against the total alkaline earths (Mg^{2+}, Ca^{2+}, and Sr^{2+}) and subtracting the Ca and Sr ions from the total. IAPSO standard seawater was used to calibrate the method and estimate precision.

Dissolved metabolites, phosphate, ammonia, silica, and organic carbon were determined by spectrophotometry. For all but the dissolved organic carbon, the procedure followed was as described in Gieskes and Peretsman (1986), together with their recommended standards. In interstitial waters containing dissolved HS the phosphate determination suffered from the precipitation of antimonyl sulfide, which imparted a brown color and precipitated to the reacting sample. This problem was alleviated by bubbling wet nitrogen through the sample for 30 min, which degassed the H_2S from the sample prior to analysis (the salinity was measured before and after to correct for any evaporation). Dissolved organic carbon ("gelbstoffe") was determined by measuring the absorbance of 1.5 mL of sample at 243.7 nm prior to the addition of the mixed phosphate reagent. This wavelength was determined by step-scanning the sample between 230 and 260 nm and calculating the wavelength of the peak of maximum absorbance.

DOWNHOLE MEASUREMENTS

Tool Strings

Downhole logging directly determines properties of *in-situ* formations adjacent to the borehole. After coring is completed at a hole, a tool string is lowered downhole on a 7-conductor cable, and each of several tools in the tool string continuously monitors some property of the adjacent borehole. Of the dozens of different tool strings commonly used in the petroleum industry, three were used on Leg 117: the seismic stratigraphic, lithoporosity, and geochemical combinations.

Two seismic stratigraphic combinations were used on Leg 117. A digital string, consisting of long-spaced sonic (LSS), natural gamma-ray tool (NGT) and phasor resistivity (DIT), was run at Site 720. An analog string, consisting of borehole com-

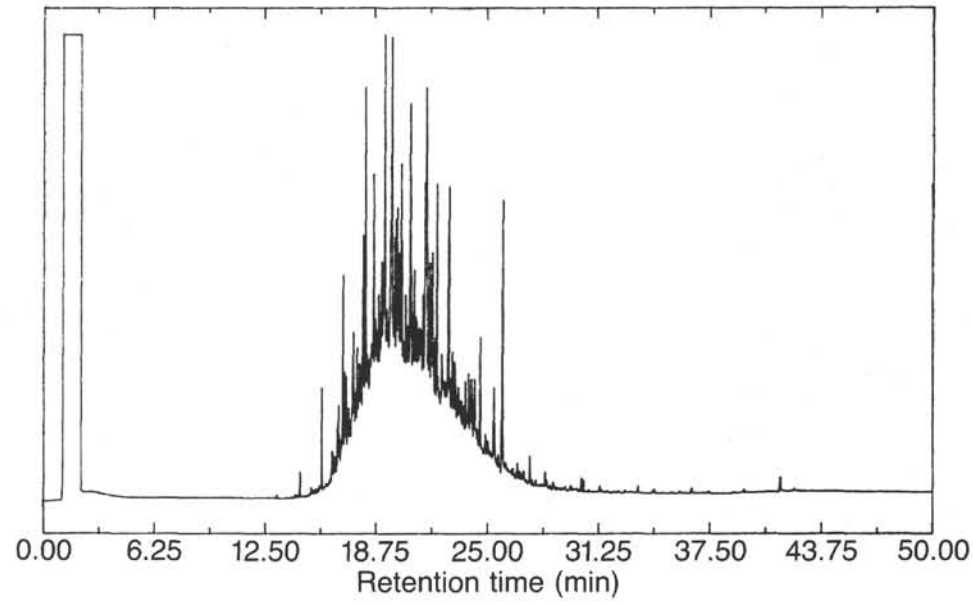

Figure 12. Gas chromatogram of an extract of acetone.

Table 7. Estimated precision ($\pm 1\ \sigma$) of interstitial-water analyses.

Species	Number	%
Alkalinity	6	1.6
Cl^-	30	0.8
Ca^{2+}	18	0.5
Mg^{2+}	24	0.4
NH_4^+	6	1.7
PO_4^{3-}	6	2.0
Si	6	0.9

pensated sonic (BHC), gamma ray (GR), and resistivity (DIL), was run at the other logged sites.

The lithoporosity combination consists of the NGT, neutron porosity (CNT-G), and lithodensity (LDT). On Leg 117 this tool string also included an accelerometer and magnetometer tool (GPIT).

The geochemical combination normally includes the NGT, aluminum clay tool (ACT), and gamma spectrometry tool (GST). On Leg 117 this tool string also included the GPIT accelerometer. At Sites 728 and 731 a modified geochemical combination was run, using a CNT-G instead of the ACT.

Logs

A brief description of logging tools run during Leg 117 is given in the following. A detailed description of logging tool principles and applications is provided in Schlumberger (1972), Serra (1984), and Timur and Toksöz (1985).

Electrical Resistivity

The dual induction log (DIL) provides three different measurements of electrical resistivity, each one with a different depth of investigation. Two induction devices (deep and medium resistivity) send high-frequency alternating currents through transmitter coils, creating magnetic fields that induce secondary (Foucault) currents in the formation. These ground-loop currents produce new inductive signals, proportional to the conductivity of the formation, which are recorded by the receiving coils. A third device (spherically focused resistivity) measures the current necessary to maintain a constant voltage drop across a fixed interval, at near-dc frequencies. Vertical resolution is around 2 m for the medium and deep resistivity devices and about 1 m for the focused resistivity.

Water content and salinity are by far the most important factors controlling the electrical resistivity of rocks. To the first order, resistivity responds to the inverse square root of porosity (Archie, 1942). Other factors influencing resistivity include the concentration of hydrous and metallic minerals, vesicularity, and geometry of interconnected pore space.

Sonic Velocity

The long-spaced sonic (LSS) tool uses two acoustic transmitters and two receivers to measure the time required for sound waves to travel over source-receiver distances of 2.4, 3.0, and 3.6 m. The borehole compensated sonic (BHC) tool uses a different source-receiver geometry, with spacings of 0.9 and 1.5 m. The data are expressed as time required for a sound wave to travel through 0.31 m of formation. First arrivals for the individual source-receiver paths are used to calculate the velocities of the different waves traveling in the formation (compressional, shear, etc.). The vertical resolution of the tool is about 0.61 m. Compressional-wave velocity is dominantly controlled by porosity and lithification; decreases in porosity and increases in lithification cause the velocity to increase.

Natural Gamma Ray

The gamma-ray (GR) tool measures the natural radioactivity of the formation. Most gamma rays are emitted by the radioactive isotope K^{40} and by the radioactive elements of the U and Th series. The gamma-ray radiation originating in the formation close to the borehole wall is measured by a scintillation detector mounted inside the sonde.

Because radioactive elements tend to be most abundant in clay minerals, the gamma-ray curve is commonly used to estimate the clay or shale content. There are rock matrices, however, for which the radioactivity ranges from moderate to extremely high values, as a result of the presence of volcanic ash, potassic feldspar, or other radioactive minerals.

Lithodensity Tool

The lithodensity tool (LDT) uses a Ce^{137} gamma-ray source to measure the resulting flux at fixed distances from the source. Under the operating conditions, attenuation of gamma rays is chiefly caused by Compton scattering (Dewen, 1983); thus, the resultant count rates can be related to the formation bulk density. A photoelectric effect index is also provided. Photoelectric absorption occurs in the energy window below 150 keV and depends on the energy of the incident gamma ray, the atomic cross section, and the nature of the atom. Because this measurement is almost independent of porosity, it can be used directly as a matrix lithology indicator. The radioactive source and detector array is placed in a that which is pressed against the borehole wall by a strong spring. Excessive roughness of the hole will cause some drilling fluid to infiltrate between the skid and the formation. As a consequence, density readings can be artificially low. Corrections can be applied by using caliper data. The vertical resolution is about 0.30 m.

Compensated Neutron Porosity

A radioactive source mounted on the compensated neutron porosity tool (CNT) sonde emits fast neutrons (4 MeV) into the formation, where they are scattered and slowed by collisions with other nuclei. When the neutrons reach a low energy level (0.025 MeV) they are captured and absorbed by atomic nuclei such as hydrogen, chlorine, silicon, and boron. The scattering cross section is the quantity that describes the rate at which neutrons are slowed. Because the scattering cross section for hydrogen is about 100 times larger than for any other common element in the crust, most energy dissipation is caused by collisions with water molecules. Therefore, a change in the number of neutrons detected at a receiver can be related to porosity. In practice, an array of detectors is used to minimize borehole or drilling fluid effects. Porosity measurements made in presence of hydrous minerals are overestimates of the true porosity. The vertical resolution of the tool is theoretically about 0.25 m, but low signal-to-noise ratio degrades this potential resolution.

Natural Gamma-Ray Tool

The natural gamma-ray tool (NGT), also called the spectral gamma-ray tool, measures the three different components (K, Th, and U) of the natural gamma-ray spectrum by differentiating between gamma rays of different energies.

Gamma Spectrometry Tool

This induced spectral gamma-ray tool (GST) consists of a pulsed source of 14-MeV neutrons and a gamma-ray scintillation detector. A surface computer performs spectral analysis of gamma rays resulting from the interactions of neutrons emitted by the source with atomic nuclei in the formation (Hertzog, 1979). Characteristic sets of gamma rays from six elements dominate the spectrum, permitting calculation of six elemental yields: Ca, Si, Fe, Cl, H, and S. As their sum is always one, they do not reflect the actual elemental composition. Therefore, ratios of these yields are commonly used in interpreting the lithology, porosity, and salinity of the formation fluid.

Aluminum Clay Tool

Aluminum abundance as measured by the Aluminum Clay Tool (ACT) is determined by neutron-induced (Cf chemical source) late gamma-ray spectrometry. By placing NaI detectors both above and below the neutron source, contributions from natural gamma-ray activity can be removed. Calibration to elemental weight percent is performed by taking irradiated core samples of known volume and density and measuring their gamma-ray output while placed in a jig attached to the logging tool (generally after logging).

Log Data Quality

Log data quality may be seriously degraded in excessively large sections of the borehole or by rapid changes in the hole diameter. Resistivity and velocity measurements are less sensitive to borehole effects, whereas the nuclear measurements (neutron porosity and natural and induced spectral gamma ray) are most seriously impaired, because of the large attenuation by the borehole fluid. Corrections can be applied to the original data in order to reduce the effects of these conditions and, generally, any departure from the conditions under which the tool was calibrated.

Different logs may have small depth mismatches, caused by either cable stretch or ship heave during recording. Small errors in depth matching can impair the results in zones of rapidly varying lithology. To minimize such errors, a hydraulic heave compensator adjusts for rig motion in real time. The heave compensator performed poorly on Leg 117; fortunately, seas were generally calm. Precise depth matching of legs with cores is not obtainable in zones where core recovery is low because of the inherent ambiguity of placing the recovered section within the interval cored.

Log Analysis

During logging, incoming data were observed in real time on a monitor oscilloscope and simultaneously recorded on digital tape in the Schlumberger logging unit. After logging, this tape was copied from 800- to 1600-bpi on the shipboard VAX computer system. The 1600-bpi tape was then read by the Masscomp computer system in the downhole logging laboratory aboard ship and reformatted to a file format compatible with the Terralog log-interpretation software package. Rather than being a "black box," Terralog is an interactive system consisting of many log manipulation and plot options. Thus, the log analysis and interpretation varied in duration and procedure for each site. Most log interpretation was carried out aboard ship; further analysis and interpretation were undertaken after the cruise, using a companion system in the Borehole Research Laboratory of Lamont-Doherty Geological Observatory.

Reprocessing of Geochemical Logs

Raw GST logs for Leg 117 are shown following the barrel sheets for each site at which the GST was run (see chapters for Sites 723, 728, and 731). Raw count rates for six elements (Ca, Si, Fe, S, Cl, and H) are obtained in real time by the Schlumberger data acquisition software. These count rates commonly exhibit some inversion interference of chlorine with other elemental count rates, which is manifest as a strong but spurious correlation between chlorine and calcium, and weaker correlations with other elements measured by the tool. This interference, which is attributable to the dominance of the induced gamma spectrum by chlorine, is unavoidable in ODP holes because the minimum pipe diameter is too small to permit use of a boron sleeve for chlorine count suppression. Most of this interference effect was removed aboard ship by standardizing each count-rate log and then removing a first-degree regression with chlorine.

The shipboard correction was obviated by post-cruise reprocessing, using a Schlumberger Elite 1000 workstation and proprietary Schlumberger software. With a revised algorithm, the gamma spectrum at each depth is inverted for titanium, gadolinium, and potassium in addition to the six elements (Ca, Si, Fe, S, Cl, and H) in the shipboard inversion. Though gadolinium is present in concentrations of only a few parts per million, its neutron capture cross section is so large that gadolinium can account for 10%–30% of the total gamma spectrum. Inclusion of these additional elements improves the quality of the overall inversion, particularly improving the accuracy of calculated cal-

cium abundance, by converting sources of unaccounted variance to signals. However, the determined potassium concentrations are less accurate than those from the NGT, and the hydrogen concentrations are less accurate than those from the neutron tool.

Data from the NGT were also reprocessed after the cruise with Schlumberger software. Shipboard real-time calculation of potassium, thorium, and uranium was based on all five recorded energy windows of the natural gamma spectrum. In the reprocessing, data from the lowest energy window are not used because this window has the highest noise level and is by far the most sensitivity to possible mud effects on the gamma spectrum. Every logged hole on Leg 117 was filled with mud.

All spectral gamma data from Leg 117 were reprocessed. In general, this reprocessing had little effect on the character of upcoming logs, but it increased estimated potassium and thorium concentrations significantly. The reprocessing degraded the quality of downgoing logs, as evidenced by an increase in log variance and decrease of replicability with upcoming logs. Apparently, with the faster logging speeds and reduced accuracy of count-rate statistics for downgoing logs, one cannot afford to discard a spectral window even if its signal-to-noise ratio is lower than that of the other four windows. Consequently, the downgoing spectral gamma logs shown in the "Downhole Measurements" sections of the site chapters are without reprocessing. The reprocessed upcoming logs shown in "Downhole Measurements" sections are in contrast to the raw upcoming logs following the barrel sheets of the site chapters.

Aluminum concentrations from the ACT require only one correction, an adjustment for variations in cable speed. Changes in logging speed affect the time lag between neutron irradiation of the formation and recording of the induced gamma spectrum because the number of induced gamma rays decreases rapidly with time. Post-cruise correction was made based on the cable speed recorded during logging. However, the small amount of ship heave during logging may make this correction less reliable in ODP holes than in land wells.

When all three Schlumberger tool strings are run, further reprocessing of geochemical logs is possible. The relative abundances of Ca, Si, Fe, Ti, Al, K, S, Th, U, and Gd are used to calculate a log of predicted photoelectric effect. The difference between this log and the actual log of photoelectric effect can be attributed to the only two major elements not directly measured, Mg and Na. Major elements are converted from volume percent to weight percent using logs of total porosity (bound water plus pore water) and density. Major elements are expressed in terms of oxide dry weight percent, based on the assumption that oxygen is 50% of the total dry weight. Site 723 was the only Leg 117 site where three-tool strings were run and, thus, for which these procedures were undertaken.

If GST data are available but not enough log types are run to permit complete solution for oxide weight percentage, one further processing step is made. Omitting chlorine and hydrogen, the yields of the other GST elements (Ca, Si, Fe, Ti, S, K, and Gd) are summed, and each is expressed as a fraction of this total yield. This procedure corrects for porosity and count rate variations. Although the absolute abundance of each element is not determined, downhole variations in relative abundance are indicated. This processing was conducted at Sites 722 and 731.

REFERENCES

Archie, G. E., 1942. The electrical resistivity log as an aid in determining some reservoir characteristics. *Pet. Technol.*, 5(1).

Barnes, R. O., 1987. ODP *in-situ* fluid sampling and measurement: a new wireline tool. *In* Mascle, A., Moore, J. C., et al., *Proc. ODP, Init. Repts.*, 110: College Station, TX (Ocean Drilling Program), 55–63.

Barron, J. A., Keller, G., and Dunn, D. A., 1985. A multiple microfossil biochronology for the Miocene. *In* Kennett, J. P. (Ed.), *The Miocene Ocean: Paleoceanography and Biogeography*: Mem. Geol. Soc. Am., 163:21–36.

Becker, K., Langseth, M. G., and Von Herzen, R. P., 1983. Deep crustal geothermal measurements, Hole 504B, Deep Sea Drilling Project Legs 69 and 70. *In* Cann, J. R., Langseth, M. G., Honnorez, J., Von Herzen, R. P., White, S. M., et al., *Init. Repts. DSDP*, 69: Washington (U.S. Govt. Printing Office), 223–235.

Berggren, W. A., Kent, D. V., Flynn, J. J., and Van Couvering, J. A., 1985a. Cenozoic geochronology. *Geol. Soc. Am. Bull.*, 96:1407–1418.

Berggren, W. A., Kent, D. V., and Van Couvering, J. A., 1985b. The Neogene: Part 2, Neogene geochronology and chronostratigraphy. *In* Snelling, N. J. (Ed.), *The Chronology of the Geological Record*: Geol. Soc. Mem. (London), 10:211–260.

Blow, W. H., 1969. Late middle Eocene to Recent planktonic foraminiferal biostratigraphy. *In* Bronnimann, P., and Renz, H. H. (Eds.), *Proceedings of the First International Conference Planktonic Microfossils, Geneva, 1967*: Leiden (E. J. Brill), 1:199–421.

Boyce, R. E., 1973. Appendix I. Physical property methods. *In* Edgar, N. T., Saunders, J. B., et al., *Init. Repts. DSDP*, 15: Washington (U.S. Govt. Printing Office), 1115–1128.

_____, 1976. Definitions and laboratory techniques of compressional sound velocity parameters and wet-water content, wet-bulk density, and porosity parameters by gravimetric and gamma ray attenuation techniques. *In* Schlanger, S. O., Jackson, E. D., et al., *Init. Repts. DSDP*, 33: Washington (U.S. Govt. Printing Office), 931–958.

_____, 1977. Deep-sea drilling procedures for shear strength measurements of clayey sediment using modified Wykeham Farrance Laboratory Vane Apparatus. *In* Barker, P., Dalziel, I.W.D., et al., *Init. Repts. DSDP*, 36: Washington (U.S. Govt. Printing Office), 1059–1068.

Carlson, R. L., and Christensen, N. L., 1979. Velocity anisotropy in semi-indurated calcareous deep-sea sediments. *J. Geophys. Res.*, 84: 205–211.

Cox, A., 1983. Magnetic reversal time-scale. *In* Harland, W. B. (Ed.), *A Geologic Time-Scale*: Cambridge (Cambridge Univ. Press), 63–84.

Dean, W. E., Leinen, M., and Stow, D.A.V., 1985. Classification of deep-sea, fine-grained sediments. *J. Sediment. Petrol.*, 55:250–256.

Dewen, J. T., 1983. *Essentials of Modern Open Hole Log Interpretations*: Tulsa (Penwall).

Dunham, K. W., 1987. Potential organic geochemical contaminants on board the *JOIDES Resolution*. *In* Boillot, G., Winterer, E. L., et al., *Proc. ODP, Init. Repts.*, 103: College Station, TX (Ocean Drilling Program), 71–74.

Espitalié, J., Madec, M., and Tissot, B., 1977. Source rock charcterization method for petroleum exploration. *Proc. Annu. Offshore Technol. Conf.*, 9:399–404.

Gieskes, J. M., and Peretsman, G., 1986. Water chemistry procedures aboard *Joides Resolution*—some comments. *ODP Tech. Note*, 5:1–46.

Hamilton, E. L., 1971. Prediction of *in-situ* acoustic and elastic properties of marine sediments. *Geophysics*, 36:266–284.

Hertzog, R., 1979. Laboratory and field evaluation of an inelastic-neutron-scattering and capture gamma ray spectroscopy tool. *Soc. Pet. Eng. Pap.*, 7430.

Johnson, D. A., Nigrini, C., and Caulet, J. P., in press. Pliocene-Pleistocene radiolarian events and magnetostratigraphic calibrations for the tropical Indian Ocean. *Mar. Micropaleontol.*

Johnson, D. A., and Nigrini, C. A., 1985. Synchronous and time-transgressive Neogene radiolarian datum levels in the equatorial Indian and Pacific Oceans. *Mar. Micropaleontol.*, 9:489–523.

Kvenvolden, K. A., and McDonald, T. J., 1986. Organic geochemistry on the *JOIDES Resolution*—an assay. *ODP Tech. Note*, 6.

Martini, E., 1971. Standard Tertiary and Quaternary calcareous nannoplankton zonation. *In* Farinacci, A. (Ed.), *Proceedings of the Planktonic Conference, II, Roma, 1970*: Rome (Ed. Technoscienze), 2: 739–785.

Matthews, D. J., 1939. *Tables of Velocity of Sound in Pore Water and in Seawater*: London (Admiralty, Hydrogr. Dept).

Munsell Soil Color Charts, 1971. Baltimore (Munsell Color).

Nigrini, C., 1971. Radiolarian zones in the Quaternary of the equatorial Pacific Ocean. *In* Funnell, B. M. and Riedel, W. R. (Eds.), *The Micropalaeontology of Oceans*: Cambridge (Cambridge Univ. Press), 442-461.

Riedel, W. R., and Sanfillipo, A., 1978. Stratigraphy and evolution of tropical Cenozoic radiolarians. *Micropaleontology*, 24:61–96.

Sanfillipo, A., Westberg-Smith, M. J., and Riedel, W. R., 1985. Cenozoic Radiolaria. *In* Bolli, H. M., Saunders, J. B., Perch-Nielsen, K. (Eds.), *Plankton Stratigraphy*: Cambridge (Cambridge Univ. Press), 631–712.

Sato, T., Takayama, T., Kato, M., Kudo, T., and Kameo, K., in press. Calcareous microfossil biostratigraphy of the uppermost Cenozoic formations distributed in the coast of the Japan Sea. Part 4: Conclusion. *Sekiyu Gijutsu Kyokaishi*.

Schaefer, R. G., and Leythaeuser, D., 1984. C_2–C_8 hydrocarbons in sediments from Deep Sea Drilling Project Leg 75, Holes 530A, Angola Basin, and 532, Walvis Ridge. *In* Hay, W. W., Sibuet, J.-C., et al., *Init. Repts. DSDP*, 75: Washington (U.S. Govt. Printing Office), 1055–1067.

Schaefer, R. G., von der Dick, H., and Leythaeuser, D., 1983. C_2–C_8 hydrocarbons from Deep Sea Drilling Project Leg 71, Site 511, Falkland Plateau, South Atlantic. *In* Ludwig, W. J., Krasheninnikov, V. A., et al., *Init. Repts DSDP*, 71: Washington (U.S. Govt. Printing Office), 1033–1044.

Schlumberger, Ltd., 1972. *Log Interpretation* (Vol. 1, Principles): New York (Schlumberger).

Schultheiss, P. J., Mienert, J., and Shipboard Scientific Party, 1988. Whole-core *P*-wave velocity and gamma ray attenuation logs from Leg 108. *In* Ruddiman, W., Sarnthein, M., et al., *Proc. ODP, Init. Repts.*, 108: College Station, TX (Ocean Drilling Program), 1015–1046.

Serra, O., 1984. *Fundamentals of Well Log Interpretation* (Vol. 1): *The Acquisition of Logging Data*: Amsterdam (Elsevier).

Takayama, T., and Sato, T., 1987. Coccolith biostratigraphy of the North Atlantic Ocean, Deep Sea Drilling Project Leg 94. *In* Ruddiman, W. F., Kidd, R. B., Thomas, E., et al., *Init. Repts. DSDP*, 94, Pt. 2: Washington (U.S. Govt. Printing Office), 651–702.

Timur, A., and Toksöz, M. N., 1985. Fundamentals of well log interpretation. *Ann. Rev. Earth Planet. Sci.*, 13:315–344.

Tsunogai, S., Nishimura, M., and Nakaya, S., 1968. Complexometric titration of calcium in the presence of large amounts of magnesium. *Talanta*, 15:385–390.

van Gorsel, J. T., and Troelstra, S. R., 1981. Late Neogene planktonic foraminiferal biostratigraphy and climatostratigraphy of the Solo River section (Java, Indonesia). *Mar. Micropaleontol.*, 6:183–209.

Wentworth, C. K., 1922. A scale of grade and class terms of clastic sediments. *J. Geol.*, 30:377–390.

Von Herzen, R. P., and Maxwell, A. E., 1959. The measurement of thermal conductivity of deep-sea sediments by a needle-probe method. *J. Geophys. Res.*, 64:1557–1563.

Yokota, T., Kinoshita, H., and Uyeda, S., 1980. New DSDP (Deep Sea Drilling Project) downhole temperature probe utilizing IC RAM (memory) elements. *Tokyo Daigaku Jishin Kenkyusho Iho*, 55:75–88.

Ms 117A-103